Numerical Investigation of Photonic Crystal Fiber based Plasmonic Biosensor for Early Detection of Cancer

A PROJECT REPORT

SUBMITTED IN PARTIAL FULFILLMENT OF THE REQUIREMENTS FOR THE AWARD OF THE DEGREE OF

MASTER OF SCIENCE
IN
PHYSICS

Submitted by:

ARHEE BHUYAN

2K23/MSCPHY/72

Under the supervision of

DR. AJEET KUMAR
Associate Professor

DEPARTMENT OF APPLIED PHYSICS

DELHI TECHNOLOGICAL UNIVERSITY

(Formerly Delhi College of Engineering)

Bawana Road, Delhi – 110042

June, 2025

DEPARTMENT OF APPLIED PHYSICS

DELHI TECHNOLOGICAL UNIVERSITY

(Formerly Delhi College of Engineering)
Bawana Road, Delhi-110042

DECLARATION

I, **Arhee Bhuyan** hereby certify that the work which is presented in the Research Work entitled in "**Numerical Investigation of Photonic Crystal Fiber based Plasmonic Biosensor for Early Detection of Cancer**" in fulfilment of the requirement for the award of the Master of Science in Applied Physics and submitted to the Department of Applied Physics. Delhi Technological University, Delhi is an authentic record of my own, carried out during a period from February 2024 to May 2025 under the supervision of Dr. Ajeet Kumar.

The matter presented in this thesis has not been submitted by me for the award of any other degree of this or any other Institute/University.

The work has been published in SCI expanded journal "Plasmonics" and some part of the work is presented in International Conference "PHOTONICS 2024" as poster presentation with the following details:

Title of the Journal Paper: Black Phosphorus based slotted D-shaped PCF SPR sensor for Cancer Detection
Author names: Arhee Bhuyan, Akash Khamaru, Ajeet Kumar
Journal Name: Plasmonics
Status of paper: Published
Date of paper received: 19th November 2024
Date of paper communication: 13th December 2024
Date of paper published: 19th December 2024

Title of the Conference Paper: Design and Analysis of Black Phosphorus layered SPR-PCF Biosensor for Detection of Cancerous Cells

Author names: Arhee Bhuyan, Akash Khamaru, Ajeet Kumar

Conference Name: 16th International Conference on Fiber Optics and Photonics

Conference Dates with venue: 12th -15th December 2024

Have you registered for the conference? Yes

Status of paper: Communicated

Date of paper communication: 10th February 2025

Place: Delhi Arhee Bhuyan

Date: 03.06.2025

SUPERVISOR CERTIFICATE

To the best of my knowledge, the above work has not been submitted in part or full for any Degree or Diploma to this University or elsewhere. I, further certify that the publication and indexing information given by the students is correct.

Place: **Dr. Ajeet Kumar**

Associate Professor

Date:

ACKNOWLEDGEMENT

I would like to extend my heartfelt gratitude to my esteemed Supervisor, Dr. Ajeet Kumar, whose steady guidance and intuitive advice has paved the path for this research work on the application of Photonic Crystal Fibers. His mentorship has been crucial in giving the direction and success of this work. My sincere thanks goes goes to Prof. Vinod Singh, Head of the Department of Applied Physics, for providing the required infrastructure and the nurturing environment for our research work.

I am deeply grateful to the committee members for their valuable feedback and constructive suggestions, which has greatly the quality of this study. I am grateful to Delhi Technological University for providing me the platform to perform this research and also the resources throughout.

A very special thanks to Mr. Akash Khamaru, a PhD scholar in our lab, for his invaluable assistance and persistent support and motivation. His encouragement has inspired me a lot throughout my research journey.

Extending my profound gratitude to all my friends and family. Their untiring love and support has been the backbone to this journey.

Arhee Bhuyan

ABSTRACT

This work proposes Surface Plasmon Resonance based Photonic Crystal Fiber for cancer detection. Both the proposed sensors are refractive index sensors that is highly sensitive towards change in refractive index of the analyte. Here the analyte used is a solution of blood cells from an infected body and a healthy body. So, by comparing the change in refractive index of both the analytes, sensitivity of the proposed sensors are determined. Fibers are simulated by the Finite element method (FEM) in COMSOL Multiphysics Software. Black Phosphorous is used as a plasmonic material along with gold and Titanium Dioxide, that significantly increases the sensitivity of the proposed sensors. Cancer infected cells refractive ranges from 1.38 to 1.41 in refractive index and that healthy cells ranges from 1.36 to 1.39 .This high sensitivity values at such minute change in refractive index displays the potential of the sensors. All the required fabrication process are suggested to show the possibility of making such sensors for real world applications.

LIST OF RESEARCH WORKS AND PUBLICATIONS

Publications related to Thesis:

✓ Journal Publication

Arhee Bhuyan, Akash Khamaru, Ajeet Kumar, "Black Phosphorus-Based Slotted D-Shaped PCF SPR Sensor for Cancer Detection" (**Published in Plasmonics, Springer on 19th December 2024**) (**SCIE-indexed journal, I.F 3.3**) https://doi.org/10.1007/s11468-024-02715-5

✓ Conference Publication

Arhee Bhuyan, Plakshi Gupta, Akash Khamaru, Ajeet Kumar, "Design and Analysis of Black Phosphorus layered SPR-PCF Biosensor for Detection of Cancerous Cells**,** photonics 2024, 12th-15th December 2024**,** IIT Kharagpur, West Bengal, India. **(Poster presented and full-length paper communicated)**

CONTENTS

LIST OF FIGURES

LIST OF TABLES

LIST OF ABBREVIATIONS

RI	Refractive Index
RIP	Refractive Index Profile
TIR	Total Internal Reflection
PCF	Photonic Crystal Fiber
CL	Confinement Loss
EMA	Effective Mode Area
ECM	Electron Cloud of the Metal
FEM	Finite Element Method
FWHM	Full Width at Half Maximum
FDTD	Finite Difference Time Domain
PDE	Partial Differential Equations
SPR	Surface Plasmon Resonance
SPP	Surface Plasmon Polaritons
PML	Perfectly Matched Layer

CHAPTER 1

INTRODUCTION

1.1. PHOTONIC CRYSTALS

From the start of human civilisation, humans are trying to eliminate the darkness. Edison's light bulb, fire, etc. are a very few ways of light sources that were thought of. We were dependent on such old light sources like incandescent bulb, fluorescent light sources even after having such high level sophisticated technologies. These light sources are known to waste 80-90% of the electrical energy input. For the improvement U.S. Academy of Sciences compiled a report citing LEDs as lighting sources will give the major impact on the economy both in saving and lighting as well [1]. Here comes the concept of photonic crystals which is very important in the making of such efficient LEDs. Semiconductors based light emitters are the most appropriate choice in the making of such LEDs. These materials are the best known materials to man which has an internal quantum efficiency of 90%. But unfortunately, only 3-20% of the light could escape the material and the remaining light was trapped inside the material (Fig-1(a)). Whereas laser diodes have developed in a tremendous manner. Many devices have shown a total efficiencies of around 50% and above. But they waste a lot of light that can be used or not be emitted, if photonic band gap principles were applied.

Therefore, a requirement for improving the ability of the effectiveness of LEDs was felt. Photonic crystals came to the picture for addressing the problem of extraction of light, altering the light generation process in the material, operating characteristics improvement of the laser diodes. Photonic crystal promises improvement both in case of LEDs and lasers. Their ability to control the flow of light, to concentrate light and to enhance the light matter interaction is very surprising [1].

The way electrons are to semiconductor crystals in the similar way photons are to photonic crystals [1]. The photons having an energy range are unable to penetrate in the crystal, and gets reflected.

1.2. MAKING OF PHOTONIC CRYSTALS

1.2.1. **Lithography**:

Through lithographic means some of the impressive progress are made with planar structures. Photolithography cannot be used for the sizes of the lattice periodically between 220-735 nm, instead electron-beam lithography is a perfect alternative. This method is used by several groups of people to generate patterns to use in the visible to near infrared red region [1]. Many groups have successfully generated triangular pattern using multiple exposer holography. This technique known as 'multiple exposer holography' is used to actually generate two-dimensional periodic structure.

1.2.2. **Masking**:

2-D photonic crystals consisting of a set of small holes is the most appropriate structure that is etched deeply in the semiconductor material. Conventional wet etching is not used as this needs an anisotropic and deep etching with a very high resolution. Selection of a suitable mask layer is very important. The solution is to generally use the resist after the development. During the etching process the resist erodes constantly, however the etch depth that can be obtained is limited, mainly for the high-resolution pattern that requires thin resists. Therefore a dielectric pattern-transfer is added for deeper etching. Using fluorine chemistry given layer can be patterned by plasma etching. Thickness chosen for this layer is ranges from 100-200 nm; the thickness of the mask decides the amount of plasma it can hold and how deep the semiconductor can be etched and the semiconductor can be etcher deeper. Thinner mask implies the thinner resist can be used to pattern, achieving a higher resolution.

1.2.3. **Dry etching**:

GaAs/AlGaAs semiconductors has a standard etch chemistry is chlorine based by using Cl_2 or $SiCl_4$. Out of all the dry etchning techniques the most appropriate method is chemical assisted ion-beam etching. Chemically assisted ion-beam etching is the most appropriate dry etching technique. It usually has a ratio greater than 20:1. A energy beam that is collimated is impinged on the sample, results in an improved RIE lag and directionality. Non selective etching or vertical sidewalls are both achieved with CH_4/H_2, it is caused by the build-up of polymer that clogs the small features. This problem is solved by using chlorine chemistry [1].

1.2.4. Electrochemistry

Electrochemistry also known as anodic etching and growth, is an alternative method to produce 2-D lattices. It has an impressive aspect ratio for both silicon and alumina. Previous researchers have closely approximated the goal of an "infinitely high" set of holes. "Infinitely high" is a term to understand in context of wavelength. Due to the generally "macroscopic" feature size of the electrochemically etched holes, these materials are known as the "microporous" silicon. Structures smaller than this is produces by technique of anodic growth.

1.2.5. Vertical Selective Oxidisation

Etching of holes and slots in a material is done to create a high refractive index contrast. Removal of material will leave the surface pierced that will make it difficult to deposit mirrors and contacts afterwards. The devices may go through premature aging because of chemical reaction in the exposed surface. Materials having this issues are removed by using the technique of selective oxidisation. The lattice produced by this technique, maintains the physical integrity of the material and hence produces an "all-solid" microstructure.

1.2.6. Membranes

The above techniques assumes that the light is confined in a "Laser-like" semiconductor heterostructure. This approach has a lot of advantages like

mechanical stability, simplicity and it allows current injection. The actual drawback of this technique is that the light is weakly confined by the limited refractive index contrast that is available with a semiconductor heterostructure, and given the opportunity, will scatter into the substrate. This loss of scattering can be minimised by designing it carefully. It cannot be completely removed unless the refractive index contrast between the cladding and the waveguide core is increased [1].

1.3. OPTICAL FIBER

An optical fiber is a hollow structured waveguide made up of dielectric material in which light can travel from one place to another i.e. information can be guided from one place to another using the phenomenon of total internal reflection (TIR). Total internal reflection is the phenomenon in which light striking at interface of two medium (e.g. water to air) is not refracted into the second medium but get reflected back into the first medium. The two necessary conditions for TIR to occur are:

a) The light must travel from a medium with lower wave speed (high refractive index) to a medium with higher wave speed (high refractive index).

b) The angle of incidence on the interface (boundaries) of the two medium must be greater than the critical angle (θ_c).

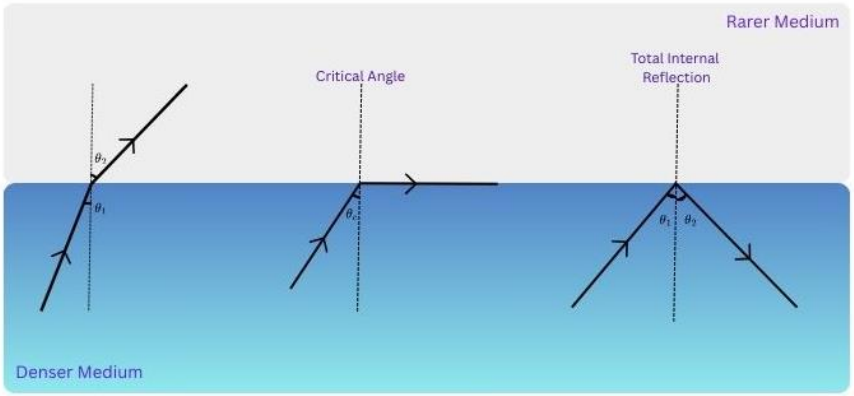

Fig. 1.1 Total Internal Reflection (TIR)

An optical fiber comprises of

1.3.1. Core

It is a high refractive index (n_1) region in an optical fiber made up of silica or any other dielectric medium. The light guidance takes place inside the core region of the fiber with the help of TIR.

1.3.2. Cladding

The low refractive index (n_2) region surrounding the core region is called cladding. Cladding is generally made up of silica or any other optically transparent material having lower refractive index than that of core.

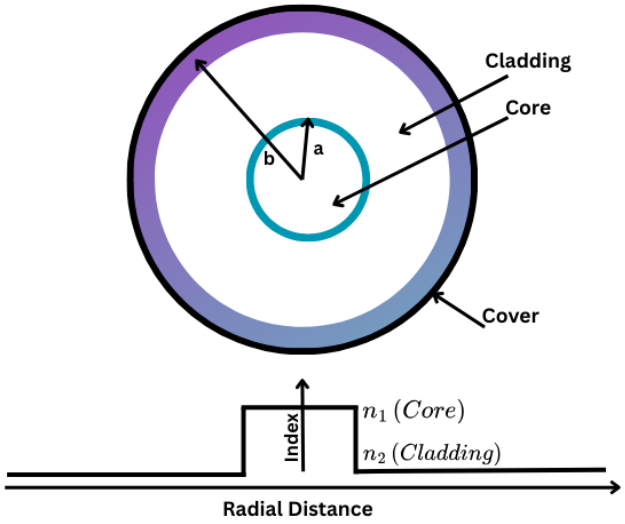

Fig. 1.2 Cladding and Core of an Optical Fiber

1.4. TYPES OF OPTICAL FIBER

Optical fiber can be classified on the basis of their structural design. Fibers are mainly classified as:

1.4.1. Single-Mode Fiber

The core diameter in such fibers is reduced to a limit such that they allow only fundamental mode to propagate through them. These fibers have the core

diameter of few wavelengths as compared to the wavelength of light propagating into the fiber. These fibers do not exhibit modal dispersion hence are more compatible for long range communications.

1.4.2. Multi-Mode Fiber

Optical fibers which allows multiple modes of light to propagate through them are known as multimode fibers. The diameter of core in multimode fibers is larger than wavelength of light propagating through them. The number of modes that can propagate through them is directly proportional to the diameter of core i.e. with the increase in diameter of core the number of propagating modes also increases and vice versa. Multimode fibers can be further classified into two categories as follows.

1.4.2.1. Step Index Fiber

The optical fibers in which the refractive index profile of core and cladding regions are constant are known as step index fibers. The refractive index of core region is higher than that of cladding region. Thus, at the interface of core and cladding regions, there is sharp and sudden decrease of refractive index. These fibers can be fabricated using Vapour phase deposition method [2].

Due to difficulties in dispersion engineering and large effective mode areas of step index fibers, they are not much used for supercontinuum generation. The schematic diagram of refractive index profile of step index fiber is shown in figure.

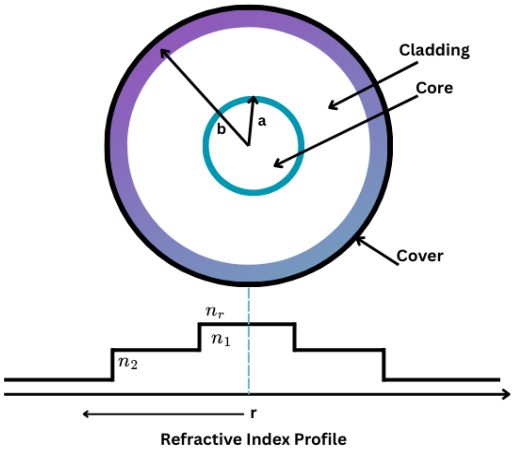

Fig. 1.3 Step Index Fiber with its Refractive Index Profile

1.4.2.2. Graded Index Fiber

The optical fibers in which the refractive index profile gradually decreases as we move from core region to cladding region are known as graded index fibers. The gradual decrease in the refractive index of graded index fibers helps in achieving low modal dispersion and hence graded index fibers are used in long haul communications. The refractive index profile for the graded index fibers (parabolic) is shown in figure.

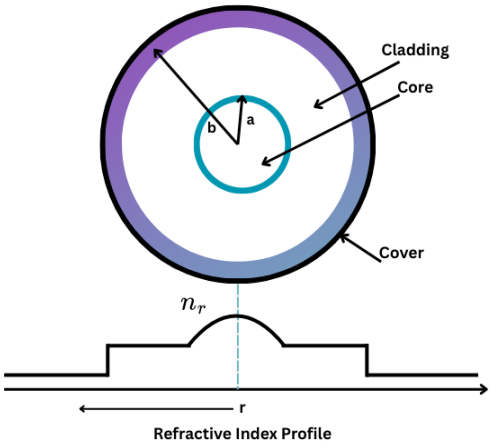

Fig. 1.4 Graded Index Fiber with its Parabolic RIP

1.4.3. Special Fibers: Photonic Crystal Fiber

Photonic crystal fibers are holey fibers which uses photonic crystals for the cladding and core. The core region is high index region and cladding consists of air holes arranged in a certain manner which reduces the refractive index of cladding region. Photonic crystal fibers are more efficient than conventional fibers as the refractive index of the core and cladding region can be changed easily either by changing the arrangement or shape of air holes in the cladding region or by altering size of air holes in the cladding region. Losses in photonic crystal fibers are also low as compared to conventional fibers. PCFs can be mainly classified in two categories.

1.4.3.1. Index Guided PCF

In index guided PCF modes of light propagate core in the same way as in conventional fibers i.e. by the phenomena of total internal reflection. The core of the fiber is made up of high refractive index material and cladding consist of air

holes with the same dielectric material as that of core. As the cladding region now has air holes in it, thus due to the presence of air holes the effective refractive index of the cladding region decreases. As the refractive index of core is higher than that of cladding region, hence the leakage of light energy to the cladding region is minimized. The refractive index profile and the fundamental mode guidance of index guiding PCF is shown in figure.

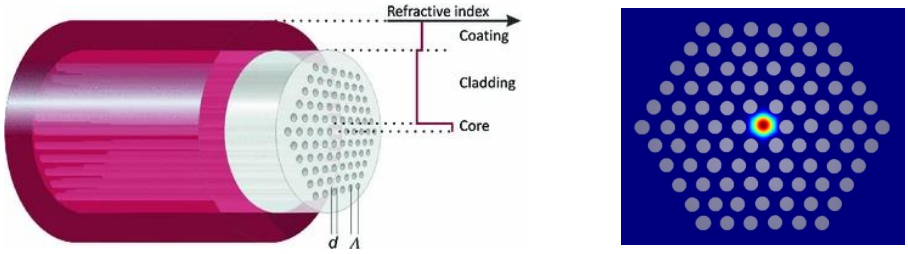

Fig. 1.5 (a) Side View of Index Guiding PCF [3]
(b) Fundamental Mode in Index Guiding PCF
[www.optics.ansys.com]

1.4.3.2. Band Gap Guided PCF

In bandgap guided PCF, the core is made hollow through which the modes of light can propagate utilizing the photonic band gap effect. This effect arises from the periodic structure of air holes in the cladding region and is analogous to the formation of band gaps 8 in solid state physics in the presence of periodic potential. The light in the core region is guided as cladding prevents the propagation of some wavelengths and effectively reflects those in the core region. The core of the fiber can be hollow i.e. air filled or can be filled with liquid or gases [4] resulting in the increase in non-linearity which can help in various non-linear applications. The fabrication of the index guided PCF is comparatively difficult but fiber can be realized by using stack and draw technique [5].

CHAPTER 2

PHOTONIC CRYSTAL FIBER

Photonic Crystal Fiber (PCF) based sensor, interferometer and grating based biosensor and resonator based biosensor [6]. PCFs are a class of optical fiber that uses a periodic structure of air holes within the cladding to confine light. This structure creates unique properties not found in traditional optical fibers, such as tailored dispersion characteristics, high birefringence, and enhanced nonlinearity [7], PCFs can be utilized for both light guiding and fluid flow channels. Due to these results samples interact significantly with light. Due to the addition of the bio-sensing, they can bind efficiently with the biomolecular targets. Intense interaction between the sample and light is achieved for the detection of the particular sample, due to the small size of the core and cladding air holes. Sensing needs very small samples of fluid volume. Small volume consumption is of great interest in chemical and biological applications.

PCFs are fabricated by using either Stack and Draw Technique or Extrusion Fabrication Process. Different types of materials are used for the fabrication of PCFs such as fluoride glasses, chalcogenide glasses, silica and polymers. These properties give rise to a large number of applications like terahertz communication, terahertz-based sensors, refractive index sensors, pressure sensors, electric and magnetic field sensor [8], super continuum generation, high-power fiber lasers, fiber components for metrology and spectroscopy, etc.

2.1. TYPES OF PHOTONIC CRYSTAL FIBER

2.1.1. Solid Core

Fiber with cladding having a lower refractive index than that of the core is a solid core photonic crystal fiber. Due to the higher refractive index of the core than that of the cladding these fibers can undergo TIR.

2.1.2. Hollow Core

Hollow core photonic crystal fiber works on a reverse theory than the solid core photonic crystal fiber. In such fibers the core is hollow acting as a defect such that a certain frequency of light pass through it called the Photonic band gap. As the core, it has a lower refractive index compared to the cladding.

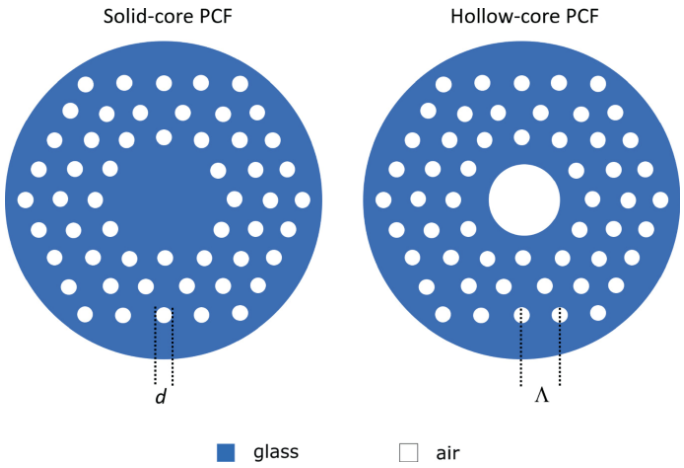

Fig 2.1 (a) Solid Core PCF, **(b)** Hollow Core PCF [9]

2.1.3. Porous core

In this case the core is porous which means the core comprises of a lot of pores or voids to be precise, which affects the propagation of light across the fiber. Different configurations of the voids such as the size, arrangements and frequency of these holes can be used to achieve different optical properties.

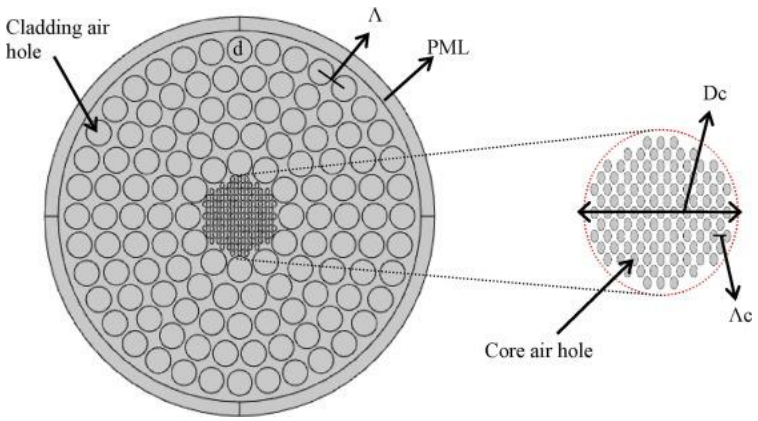

Fig 2.2 Porous Core PCF [10]

2.2. ADVANTAGES OF PCF

PCFs are known for its tunability in optical properties which helps in precisely controlling the propagation of light. Different design of the crystal lattice can help the researchers to obtain different optical properties such as birefringence, dispersion, nonlinearity etc. PCFs are compact in size and light in weight. Some fibers are polarization maintaining where the is to have specific control over the polarization, and PCFs serves the purpose. PCFs are already known to work on the principle of TIR. But they also perform on guiding mechanism which are commonly used in multiple fields such as nonlinear optics.

2.3. FABRICATION

PCFs have a very complex design. Now, the present world is full of different new technologies and advancements that allows comparatively easier fabrication of such difficult result. Various ways are used in the fabrications of PCFs such as sol-gel [11], extrusion [12], stack and draw [13], gas- pressurization, capillary stacking and 3D printing [14]. Different types of air holes such as elliptical, rectangular, circular etc. are designed by this new technology called 3D printing.

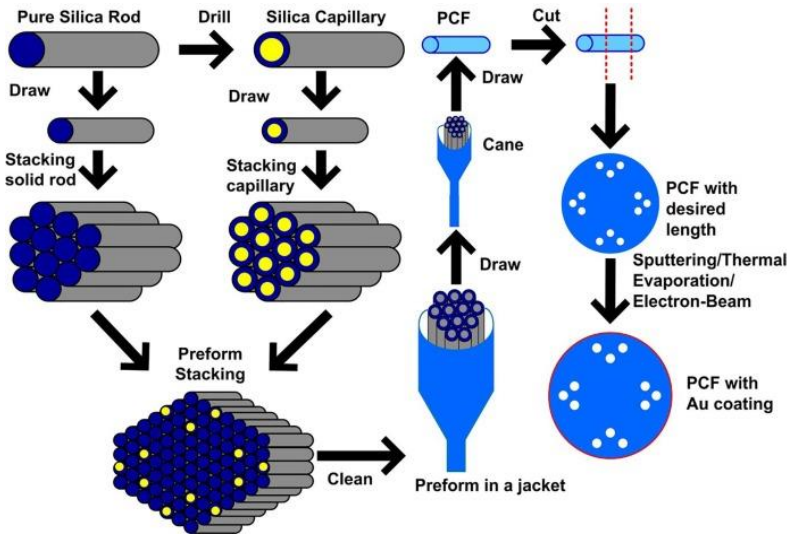

Fig 2.3 Stack & Draw Fabrication Method for PCF Sensors [15]

CHAPTER 3

SURFACE PLASMON RESONANCE AND IT'S ASSOCIATION WITH PCF

3.1. SURFACE PLASMON RESONANCE

When light travels through a thin metal film, like gold or silver, the electrons at the metal surface starts to oscillate collectively in response to the light. This oscillation of electrons is called a "surface plasmons".When the natural frequency of these oscillations matches the frequency of the incident light, it is called "resonance". When a light beam traveling from higher refractive index and hits the interface of a lower RI material. Due to total internal reflection (TIR) the light bounces back to the material with higher refractive index. This reflection of light to the higher refractive index is prevented by applying a thin layer of a conducting metal like silver, gold etc. Evanescent wave is generated as a small part of the reflected light is converted into electric field. The free electrons at the metal surface, known as **Surface Plasmons (SPs**) interacts with these evanescent waves as they penetrates through the metal surface. Electrons get excited as the momentum of the SPs and the light photons are equal in magnitude and direction at a given incident energy. These SPs as soon as they interact with light photons starts oscillating and resonating, producing **Surface Plasmon Polaritons (SPP)**. SPPs combines electromagnetic waves (polaritons) with the oscillation of charged particles (SPs) in the metal with in the dielectric or air, as shown in Fig. 3.1. This free charged particles having resonate oscillation in metals at the metal–air interface or metal–dielectric is known as SPR. As SPR is generated by a portion of light, therefore not all the light incident on the surface can be said to have completely reflected. So there is always a decrease in the intensity of the reflected light as SPR appears.

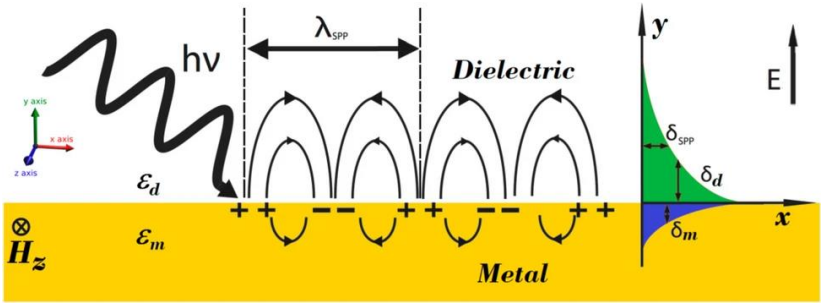

Fig 3.1 Schematic View Surface Plasmons Travelling along a Metal-Dielectric Boundary [16]

3.2. SPR BASED PCF SENSOR

Surface plasmon resonance (SPR)-based sensors have recently been designed and developed for applications in the area of medical diagnostics, biological sensing, and environmental monitoring. Due to the minimal size of the PCF core and air holes in the cladding, the intense interaction between the sample and light, sensing needs very small samples of fluid volume. The consumption of volume of sample is extremely small. Small volume consumption is of great interest in chemical and biological applications. Previously there was a sensor i.e., prism-based SPR sensors, which have drawbacks such as bulkiness, complex design, massive cost, and limited reliability. To overcome these drawbacks, PCF-based SPR sensors have grown more dominant in the field of optical sensing due to their design flexibility.

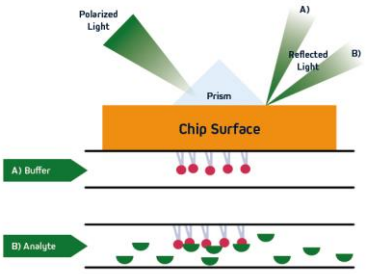

Fig 3.2 Prism based SPR Sensor [www.jacksonimmuno.com]

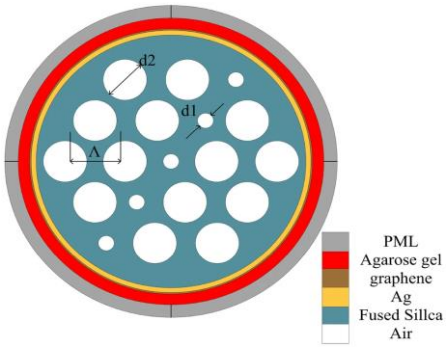

Fig 3.3 Example of SPR based PCF Sensor [17]

The prism is replaced by the fiber in the PCF-based SPR sensor. The excitation of SPs is created by the fiber coupling instead of the prism coupling. In the figure, we have a PCF based SPR sensor where analyte works as the lower refractive index material and fused silica as the higher refractive index material.

The main benefits of adopting PCF-SPR sensors are their large detection range, improved light confinement, adjustable dispersion, compact size, and extremely sensitive characteristics. A PCF-SPR sensor's sensitivity is heavily dependent on plasmonic materials such as silver, gold, aluminum, copper, bismuth, and palladium.

In comparison to other plasmonic materials, gold (Au) exhibits high chemical stability.

3.2.1. Advantages of SPR based PCF Sensors

SPR based PCF sensors are known to enhance light matter interactions, which leads to a more efficient energy transfer and better sensitivity in a lot of devices. Light propagation through these sensors obeys photonic band gap effect or the modified TIR. We can control the light propagation through the sensor just by altering the air hole geometry and altering the number of rings. These sensors can be incorporated in microscales as they are very compact. By optimizing PCF SPR geometry, one can achieve optimum evanescent fields due to it's flexibility in design. For example by using different types of PCF SPR sensors such as octagonal, hexagonal, square, hybrid, etc. the core guided leaky mode propagation can be controlled. Propagation of light in single mode can be obtained by optimizing the core-cladding diameter and propagation, which results in sensitivity enhancement.

3.2.2. Disadvantages of SPR based PCF Sensors

These sensors are very difficult to build due to their complex structure. They also very fragile and delicate. These makes them very expensive in terms of manufacturing. Integration of such sensors are also a very big issue to overcome. They are very sensitive they get easily influenced by the environment. The data interpreted by such sensors are very complicated as well

CHAPTER 4

PLASMONIC MATERIALS

As discussed earlier the generation of surface plasmons, and the way they are responsible for the SPP modes of the sensor. These plasmonic materials are some metal-like materials that is responsible for the interaction between the light and the electrons of the metal.

4.1. GOLD

Gold and silver are the most known and common plasmonic material due to their unique optical properties. When the free electrons of the metal is exposed to light it tends to interact with it and collectively oscillates at certain wavelengths. This leads to the phenomenon discussed earlier known as Surface Plasmon Resonance. Use of such plasmonic material results in strong absorption and scattering of light. Making them useful in different types of applications such imaging, bio sensing, etc.

4.2. TITANIUM DIOXIDE

TiO_2 are also considered as one of the prominent plasmonic materials. They does the same functioning as any other plasmonic material like gold or silver. As a result they are used in such sensors to enhance the sensitivity. But also have a unique adhesive property that enables them to be used as a binding element between the fiber and any other plasmonic material like gold.

4.3. BLACK PHOSPHORUS

One of the 2-D plasmonic material that amazing optical and electrical properties including high charge carrier mobility, smaller work function, binding of molecules is better on the sensor's surface [18] and direct band gap. BP is known for enhancing the sensitivity of a sensor as at specific wavelengths it can interact with light due to its property of direct bandgap [19]. Transmission of signal is faster and efficient resulting in quick response and enhanced sensitivity as its charge charrier mobility is very high. Smaller work function makes it easier for the incident electrons to excite the surface electrons. It can tightly bind the molecules on its surface as a result it plays an important role in binding biological molecules like DNA, Chemical analytes, Blood cells etc., which eventually increases its bio sensing properties. As it is a 2D plasmonic material it has a very minute thickness of 0.53nm, so to make it work multiple layers of BP is used on the sensor. Such small layers of BP are made by different processes such as Pulse Layer Precipitation, Liquid Peeling, Mechanical Peeling etc. Mechanical peeling is used most commonly where thin layers of BP are extracted of a bult material using some tools. This is cost friendly method and requires no big equipments. In liquid peeling a large piece of BP is kept in a liquid and Ultrasound waves are projected on it resulting in the projection of a large quantity of such thin BP layers. BP is used in SPR based PCF sensors for enhancement of its sensitivity, biomolecule detection, clinical applications, environmental monitoring, it doesnot let the plasmonic materials to get oxidized.

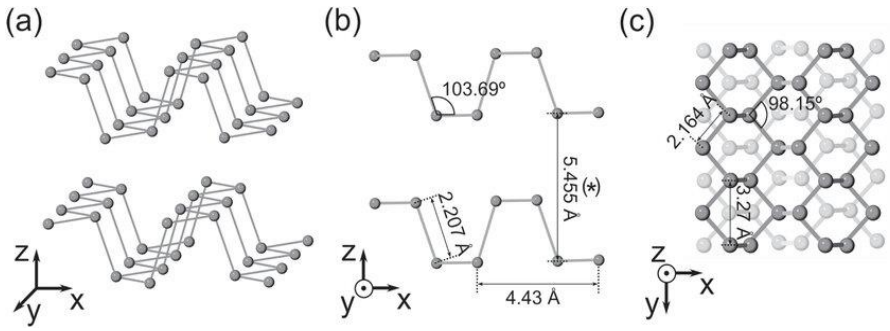

Fig 4.1 (a) 3D Representation. **(b)** Lateral View. **(c)** Top View of a 0.53nm Thin BP Layer [20]

CHAPTER 5

BIOSENSING APPROACH

The body is made up of millions of microscopic cells, each of which functions as a completely different living organism. Every single cell in our body works collectively with every other cell to form our tissues and organs. An illustration of this cooperation can be seen in the process by which cells divide. They then begin to regenerate when it becomes necessary to fix damaged or dead cells. When the process of cellular replication becomes unregulated, cancer develops. Each cell has a nucleus and the nucleus contains a huge bunch of chromosomes, whereas these chromosomes are made of genes in the form DNA strands containing coded messages that guide the cell about the work they will perform. And this is how the information of the presence of dead cells reach the brain and the cells undergoes the process of cell division [21]. During cell division mutation occurs i.e., when due to smoking or any other external factor this process of cell division gets mislead and without any instructions cells starts to grow abruptly. Forming a lump known as cancer. This is how cancer starts in the body, stays and grows without the host knowing. And as soon as it is discovered it is already in a stage where no treatment can help with the recovery. Cancer is actually growth of cells in an abnormal way which changes the usual gene replication and eventually it becomes a multiple cell system that dis-balances the cell replication in the body. It becomes such a huge cell group that it can invade any tissues in any parts of the body. It can then infect the entire organ system, causing a painful death of the host [21].

So, early detection of cancerous cell is one of the most talked topic. Generally, people can go for MRI (Magnetic Resonance Imaging), PET-CT (positron emission tomography-computed tomography), Biopsy, X-ray, CT scan etc. to regularly monitor cancerous presence in the body but they have a list of disadvantages like slow, complicated and inefficient procedures, with a lot of radiation exposer, and need of a lot of trained people to operate equipment making it more and more expensive.

Sensing techniques for detection of cancer over the years have evolved a lot. Some of them are Colometric biosensors; Fluorescence based biosensor; Resonance based optical sensing such as SPR and LSPR based sensing; Fibre based sensor such as PCF(Photonic Crystal Fiber) based sensor, interferometer and grating based biosensor and resonator based biosensor. Among all these SPR sensors are considered very efficient due to its sensing technique and high sensitivity toward its analytes [22]. So in this designed biosensor we are using a combination of Photonic Crystal Fiber (PCF) and Surface Plasmon Resonance (SPR) to detect early cancer cells in the body.

The infected counterpart of the healthy cells shows an increase in refractive index (RI) as the protein content in the nucleus of the infected cell increases. Cancer cells have many types. Skin cancer (Basal Cell), Blood Cancer (Jurkat), Adrenal gland cancer (PC-12), cervical cancer (HeLa cell), Breast Cancer (type 1 & 2) etc. The RI of healthy Basal cell, Jurkat, PC-12, HeLa cell lies between 1.36 to 1.39. Whereas, the infected counter part of these cells shows an increase in RI and lies within 1.38 to 1.41 [23, 24, 25]. These healthy and infected cell forms the sample analyte for our analysis and based on their RI difference we will calculate the sensitivity of the infected cell with respect to the healthy cell.

CHAPTER 6

SIMULATIONS AND COMSOL MULTIPHYSICS SOFTWARE

6.1. SIMULATION

In the recent time specialized softwares are used for computational simulations to evaluate the initial analysis before physically fabricating it. Different Multiphysics software such as RP Fiber, COMSOL Multiphysics, Ansys Multiphysics are used for such purposes. These analysis helps us to be aware of the performance of the designed fiber in various altered conditions to know make the most out of it. These softwares gives us an insight on different possibilities of fiber that can be designed which might not be feasible to fabricate at the moment providing valuable guidance for future developments. This way thorough research can be done on the reliability on an innovative fiber design before it fabrication that makes it very reasonably helpful for practical uses.

6.2. COMSOL MULTIPHYSICS SOFTWARE

COMSOL Multiphysics is a finite element analysis. As the laws of physics for time-dependent and space-dependent are generally expressed in partial differential equations (PDEs). But of various geometries and problems theses PDEs are not possible to be solved by analytic methods. Instead, based on some discretization an approximation of such equation can be created. This way they are approximated with some numerical model equations that are solved using numerical methods. These solutions are the approximation of the real solution to the PEDs. These approximations are generally commuted by Finite Element Method (FEM).

COMSOL Multiphysics software is a solver, and simulation software package for various physics and engineering applications, especially coupled phenomena and multi-physics. The software facilitates conventional physics-based user interfaces and coupled systems of partial differential equations (PDEs). COMSOL provides an IDE and unified workflow for electrical, mechanical, fluid, acoustics, optics and chemical applications. Besides the classical problems that can be addressed with application modules, the core Multiphysics package can be used to solve PDEs in weak form. An API for Java and LiveLink for MATLAB and LiveLink products for major CAD software can be used to control the software externally. An Application Builder can be used to develop independent custom domain-specific simulation apps. Users may use drag-and-drop tools (Form Editor) or programming (Method Editor). COMSOL server is a distinct software for the management of COMSOL simulation applications in companies. Several modules are available for categorization according to the applications areas of Electrical, Mechanical, Fluid, Acoustic, Chemical, Multipurpose, and Interfacing.

Fig 6.1 COMSOL Multiphysics Software

6.3. NUMERICAL ANALYSIS

Various types of mathematical equipments are available in these simulation software having advanced algorithms to evaluate fiber performances. Some of them are listed below:

6.3.1. Finite Element Method:

This method is used to obtain approximate solutions through numerical techniques for boundary value problems for partial differential equation (PDE) and also for solving integral equations. It converts complex problem into smaller components called finite elements and achieves the required solution. The entire physical domain is parted into finite numbers of elements, and are interconnected at nodes. This process is called meshing.

6.3.2. Finite Difference Time Domain Method:

FDTD is a method developed in the 1920 by A. Thom for simulations of one, two, three dimensional models. These method was previously used to solve hydrodynamic problems. By using central difference approximations FDTD changes differential equations into difference equations. Iteratively these difference equations are solved in an advanced manner. Within the solution region the value of these dependent variables at a defined points are known by the neighbouring points.

6.4. PROPERTIES DEFINING A PCF

PCF is designed by various properties and parameter that are used in simulations Some of them are listed below:

6.4.1. Effective Mode Index

An average refractive index is maintained by the PCF due to its design, when light travels through it. Effective mode index is actually the average refractive index. Mathematical representation of effective mode index is shown below [26]:

$$n_{eff} = \frac{\beta}{k_o} \tag{6.1}$$

6.4.2. Confinement Loss

Generally PCFs are designed in a way such confinement of radiation is maximum at its core. But due to various reasons light scatters out of the core i.e., radiation escapes the core and a confinement loss is obtained. Confinement loss is calculated by the given equation[27]:

$$Loss\left(\frac{db}{cm}\right) = 8.686 \times \frac{2\pi}{\lambda} \times Im\left(n_{eff}\right) \times 10^4 \qquad (6.2)$$

Here k_o is the propagation constant, $l_m(n_{eff})$ is the imaginary part of the effective RI.

6.4.3. Effective Mode Area

Effective mode area refers to the key zone where sensing is performed. Effective mode area attributes the spatial distribution of the guided optical mode. It is given by [28]:

$$EMA = \frac{(\iint |E|^2 dxdy)^2}{\iint |E|^4 dxdy} \qquad (6.3)$$

6.4.4. Effective material loss

It refers to the material loss due to absorption of material and scattering between the cladding and core of the fiber. It helps to determine the amount of light absorbed by a fiber. This is the ratio of the integral of the dielectric material of the fiber to the integral of the cross section of the entire fiber, which is [29]:

$$\alpha_{eff} = \sqrt{\frac{\varepsilon_0}{\mu_0}}\left(\frac{\int_{mat} n_{mat}|E|^2 \alpha_{mat} dA}{\left|\int_{all} S_z dA\right|}\right) \qquad (6.4)$$

CHAPTER 7

BLACK PHOSPHORUS-BASED SLOTTED D-SHAPED PCF SPR SENSOR FOR CANCER DETECTION[1]

7.1. Introduction

Our body has millions of cells, every one of which is a microscopic unit that is both autonomous and fully functional on its own. Together, these cells form tissues and organs which enable the body to perform its functions. One of their most important functions is to regenerate, which they can do by cell division, in order to replace dead or damaged cells. This process is controlled and regulated, but when this regulation is broken because of some mutation, mostly because of some harmful external influence like smoking, these cells start dividing without control, and this leads to cancer [21, 30, 31] . When we talk about cancer, it is about "out of the norm' uncontrolled cell growth which interrupts cell interplay between injuring white blood cells synthesis and organ disposition, resulting in the disarray of organs, severe damage to the body systems and alter rate of functionality with great chances of death.

The deadliest disease requires early diagnosis. Early detection is very important for cancer. Existing detection methods like MRI, PET-CT, biopsy, X-ray, and CT scan are used regularly but all have major limitations. Some of them include being complex [32], time intensive [33], costly, heavy on radiation [34], and necessitting specialized healthcare professionals . This need has spurred the development of newer biosensing technologies aimed at improving the efficiency and sensitivity of cancer detection.

[1] A part of the results presented in this chapter have been reported in a research publication: Bhuyan, Arhee, et al. "Black Phosphorus-Based Slotted D-Shaped PCF SPR Sensor for Cancer Detection." *Plasmonics* (2024): 1-13.

Colorimetric biosensors, fluorescence-based biosensors and other types of sensors with grating and resonator-based instruments [6] as well as SPR have been developed. Among all these sensors, surface plasmonic resonance (SPR) based sensors are considered very efficient due to its label-free sensing mechanism and deliver higher sensitivity toward its analytes [22].

Superlattice structures (SS) occur when light interacts with thin films of metals like gold or silver, producing an evanescent wave that interacts with the free electrons oscillating on the surface of the metal, which creates surface plasmons (SPs). Surface plasmon polaritons, or SPPs, are created and oscillate in Electron Cloud of the Metal (ECM) when the incident light matches the oscillation frequency. The energy of the SPPs is proportional to the amount of reflected light, hence a decrease in light intensity indirectly indicates an increase in plasmonic energy, making it possible to precisely identify the medium's SPR. These conditions are known to oscillate with the ingoing biosystem, which makes probing efficient for multi-purpose biosensing applications.

The use of PCFs also improves the efficiency of SPR sensors. They consist of a singular crystal containing physical channels along its whole length which allow light to propagate perpendicular to the fiber axis. These structures change energy distributions in light for non-linear optical applications [7]. They allow this with high refractive index and low friction which PCFs possess. The air gaps, together with the low-friction material, can also reduce the amount of liquid that needs to be tested, which is very important in medicine.

New designs of the PCF-SPR sensors have made it much easier to detect cancer. Different researchers have used different shapes of air holes, core structures, and even gold as plasmonic materials for their designs.

The sensor discussed within the text integrates gold, titanium dioxide (TiO_2), and black phosphorus (BP) as cloaking or plasmonic materials. In this case, gold was used due to its biocompatability, stability, and resilient corrosion [35], whereas TiO_2 holds the role of an anchor layer. BP is a new 2D material and further enhances sensor performance owing to its direct bandgap, tunable properties, elevated charge

carrier mobility, and strong molecule binding. These properties greatly enhance sensor sensitivity and response time [18, 19].

Each layer of BP with a thickness of 0.53 nm is multiplied to evaluate its influence on SPR response, or more generally how the sensitivity shifts with refractive index changes. Detection is designed for differentiating healthy cells and cancer-invaded tissues by means of RI comparison (Refractive Index). It's well known that cancer cells usually have higher RI values compared to normal ones because of enhanced protein content within the nucleus. Basal, Jurkat, HeLa, and PC-12 are well known healthy cells which have RIs in a range of 1.36 to 1.39 while their infected counterparts will have range from 1.38 to 1.41 [23]. It is these changes in RI that enables the proposed biosensor to achieve specificity and sensitivity.

7.2. DESIGN OF PROPOSED PCF BASED SPR BIOSENSOR

Figure 1 is the cross -sectional demonstration of the proposed biosensor. Different geometric parameters were chosen and placed in a way to create a passage for the interaction between core mode and the SPP mode of the sensor. In this designed sensor, two types of air holes are used, first is oblong air holes and second one is circular air holes. The PCF consists of two sets of oblong air holes: one has a height and width defined as H and W whereas the other slanted oblongs has same width and but height attains the magnitude of H'=1.35×H. The slanted oblongs are at an angle of 60º with each other. Therefore, as to direct the evanescent field to the plasmonic layers (Gold-TiO_2), the first type of oblong air holes are placed in a horizontal manner. Smaller air holes having diameter (d_c) are placed near the vicinity of the core to prevent any extent of leakage of light. The thickness of TiO_2 (t_{Ti}) used is 12 nm for the initial analysis and similarly gold layer has a thickness (t_g) of 50nm. Here, seven layers of BP is used each of thickness 0.53 nm united giving a total thickness of 3.71 nm to initiate the investigation.

The series of plasmonic layers over the PCF are as TiO_2, then gold (Au) over which thin films of BP are layered. TiO_2 is known to enhance the sensitivity by behaving as an adhesive between the fiber and gold layer. The bio-sample analyte is injected over the gold layer using "selective filling approach" and then a

Perfectly Matched Layer (PML) layer is added. The main purpose of adding PML to prevent any reflected radiation to be scattered.

A concentration of 30% - 70% is for healthy cells and 80% of concentration is used for infected cancerous cells in the analyte for detection. Table 7.1 shows the refractive indices of the healthy and the infected cells.

Table 7.1
Refractive Index of Various Cancerous Cell with their Cancer Types and References.

Cancer Type	Name of the cell	Refractive Index of healthy cell	Refractive Index of infected cell	References
Skin	Basal cell	1.360	1.380	[24, 25]
Blood	Jurkat	1.376	1.390	
Adrenal gland	PC12	1.381	1.395	
Cervical	HeLa	1.368	1.392	
Breast cancer-Type1	MDA-MB231	1.385	1.399	
Breast cancer-Type 2	MCF7	1.387	1.401	

For the fundamental material, the proposed sensor is composed of fused silica. It is crucial to determine the refractive index of fused silica which is done be using the known wavelength-dependent Sellmeier Equation, which states a relationship between wavelength and the refractive index, and helps to find the refractive index of fused silica at different wavelengths. The equation of Sellmeier equation is given as [36]:

$$n(\lambda) = \sqrt{1 + \frac{0.696163\lambda^2}{\lambda^2 - 0.0046791486} + \frac{0.4079426\lambda^2}{\lambda^2 - 0.0135120631} + \frac{0.8974794\lambda^2}{\lambda^2 - 97.934003}} \quad (7.1)$$

λ here represents the optical wavelength (in μm) and n(λ) represents the refractive index of fused silica.

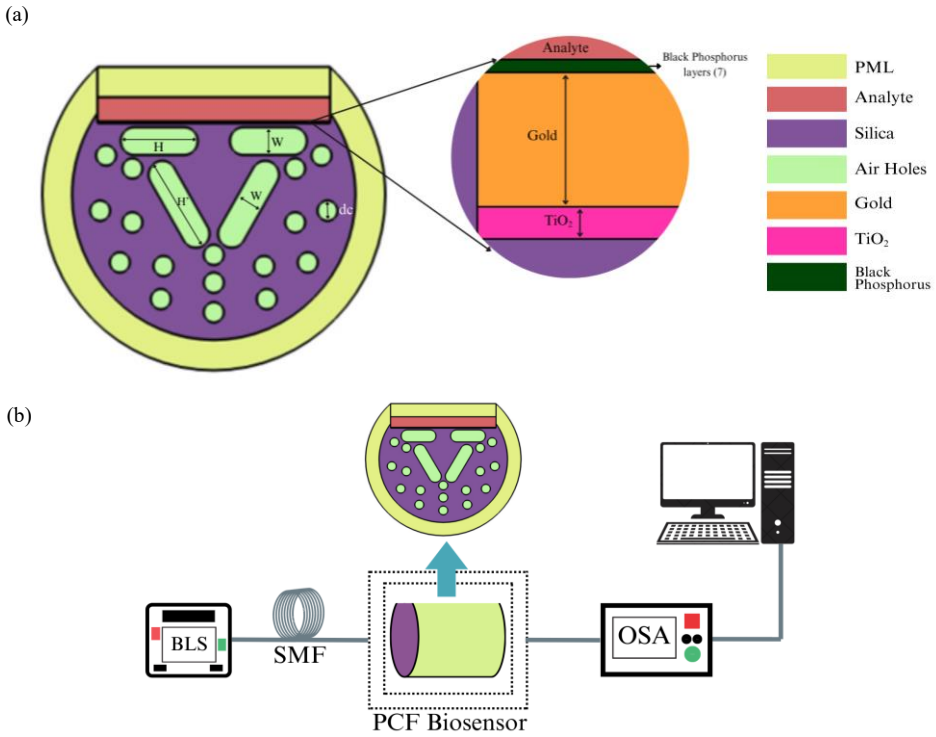

Fig.7.1 (a) Proposed PCF SPR Bio-Sensor, **(b)** Proposed Experimental Setup of the Proposed PCF SPR Sensor

Drude–Lorentz model is used here to compute the dielectric constant of gold. The Drude-Lorentz model expression is as follows [37]

$$\varepsilon_{Au} = \varepsilon_{\infty} - \frac{w_D^2}{w(w + j\gamma_D)} - \frac{\Delta\varepsilon . \Omega_L^2}{(w^2 - \Omega_L^2) + j\Gamma_L w} \quad (7.2)$$

Here, ε_{Au} represents permittivity of gold, $w = 2\pi c/\lambda$ is the angular frequency, where c is the speed of light. ε_{∞}= 5.9673, $w_D/2\pi$ = 2113.6 THz, $\gamma_D/2\pi$ = 15.92 THz, $\Omega_L/2\pi$ = 650.07 THz, $\Gamma_L/2\pi$ = 104.86 THz, $\Delta\varepsilon$ =1.09. The refractive index of TiO_2 is determined by the following equation [8]

$$n_{TiO_2} = \sqrt{5.913 + \frac{2.441 \times 10^7}{\lambda^2 - 0.803 \times 10^7}} \quad (7.3)$$

Here, n_{TiO_2} is the refractive index of TiO_2 and λ represents optical wavelength.

The refractive index of Black Phosphorous used in the sensor is measured with the help of the polynomial fitted equation [38]

$$n(\lambda) = A + B\frac{10^4}{\lambda^2} + C\frac{10^9}{\lambda^4} \quad (7.4)$$

$$k(\lambda) = D \times 10^{-5} + E\frac{10^4}{\lambda^2} + F\frac{10^9}{\lambda^4} \quad (7.5)$$

Here n(λ) is the real part, and k(λ) is the imaginary part of the refractive index, and A= 3.57, B=6.79, C=39.99, D=3206, E=0.521, F=10.26 are constants.

7.3. FABRICATION POSSIBLILITIES FOR THE PRESENTED SENSOR

The proposed PCF SPR sensor can be fabricated through procedures, such as stack-and-draw, injection molding as well as through sol-gel casting, etc. Stack and Drawing is the most used method for the fabrication because of its versatility and as it has the most inexpensive casting [39]. Stack and draw, sol–gel methods, capillary stacking are used for making fibers with circular air holes. A preform is generated by stacking a small length capillary with a known diameter into a larger diameter glass tube. Then cane is formed with the help of the preform, and a fiber having a definite diameter draws the cane into it. By shutting one end of any air-holes of the cane, air hole size can be changed. On the other hand, 3D printing, and extrusion methods have the potential to fabricate complex airhole (rectangular, oblong) within PCF structures. The previous research works had already proposed rectangular and oblong air holes with their fabrication techniques and feasibility [40, 41]. Thermal evaporation, Radio frequency sputtering, Chemical Vapour Deposition (CVD), Wet Chemical Deposition are the different methods may be used to deposit thin layers of metals like TiO_2 and gold [42]. CVD technique may be preferred for generating homogeneous metal layer with nm-range thickness

[43]. BP is fabricated using various techniques like mechanical exfoliation, liquid-phase exfoliation, electrochemical exfoliation etc. [44]. Using selective filling approach, analyte or the cell samples can be filled over the plasmonic layer into the sample channel [45]. The discussion covers all the processes and ways by which the proposed biosensor can be fabricated.

7.4. DISPERSION RELATION OF THE BIOSENSOR

The COMSOL Multiphysics software is employed for stimulating the SPR-PCF sensor using FEM (Finite Element method). FEM works with the Maxwell's equations to get the real and imaginary parts of the effective modal index (n_{eff}). The real part of n_{eff} describes the guided light modes (core and SPP modes). Whereas the imaginary part does the analysis over the losses incurred in the fiber. The confinement loss (CL) can be obtained by te previously explained equation 6.2.

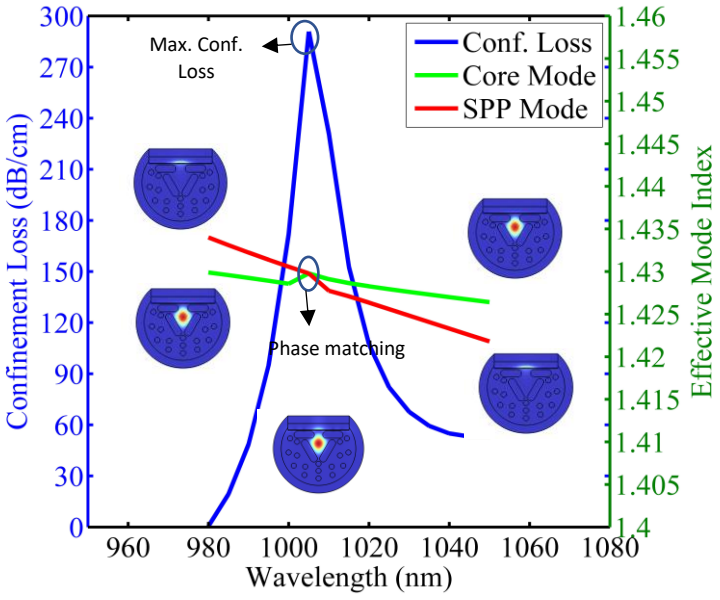

Fig. 7.2 Dispersion Curve for the Core and SPP Mode for PC12 Cancerous Cells

Dispersion relationship is taken in the y-polarisation as all the plasmonic materials lies on the top of the sensor. Figure 7.2 shows the respective core mode, SPP mode and SPR mode. The dispersion relationship between core mode and SPP

mode is also shown in fig. 7.2. In the figure, n_{eff} is marked on the right side and confinement loss is marked on the left side. The blue curve is taken in the range from 980 nm to 1050 nm that corresponds to the confinement loss. Whereas, the n_{eff} for the core and the SPP modes are denoted by the light green and the red line respectively over a range of wavelengths. The figure provides information that the peak for the confinement loss of the core mode is arrived as 290 dB/cm at 1050 nm, and both the curves for real part of the n_{eff} for core and SPP mode meets at the exact same wavelength. The point at which both these curves meet each other is known as the phase-matching position and simultaneously maximum loss observed that defines the resonance (SPR) condition. At that particular point, maximum energy is transferred from the core mode to the SPP mode, and indicates coupling between both the modes.

To evaluate the wavelength sensitivity of any cell the following equation is used [47]

$$S_\lambda \left(\frac{nm}{RIU}\right) = \frac{\Delta\lambda_{Peak}}{\Delta n_a} \tag{7.6}$$

Here, $\Delta\lambda_{Peak}$ represents the difference between the peak wavelengths of the healthy and the infected cells, Δn_a represents the difference in the refractive index between the healthy and the infected cell.

7.5. RESULT AND DISCUSSION OF THE PROPOSED PCF SPR SENSOR

7.5.1. Optimisation of the Plasmonic Materials and Geometrical Parameters

The optimisation of the structural parameters of different constituents involved in the proposed slotted PCF to be done in this section. Therefore, it is ideal to investigate different values of the parameters that can provide maximum sensitivity. Here, PC-12 (Cervical Cancer) is taken as the base cancer type for optimising the structural parameters, where 1.381 and 1.395 are the refractive index of normal and the infected cell for PC-12. The respective change in the refractive index is 0.014.

7.5.1.1. Gold (Au) Thickness Optimization

The given study given study conducted about the effects of thickness of gold (t_g). The gold thickness hugely affects the sensing performance of the sensor. The optimal thickness of the gold is determined by varying it in the range of 35 nm-55 nm at a difference of 5 nm. Figure 3 depicts the graphical representation of confinement loss versus the wavelength with the varying thicknesses.

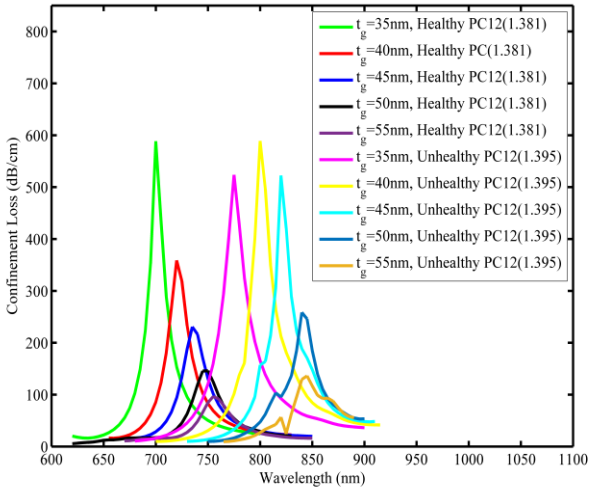

Fig. 7.3 CL Spectra for Various Gold Thicknesses (t_g) at RI of 1.385 and 1.391

Table 7.2
Optimization of Thickness of Gold Layer (t_g)

t_g (nm)	Max. CL (Normal cell) (dB/cm)	Max. CL (Infected cell) (dB/cm)	ΔWL (nm)	Sensitivity (nm/RIU)
35	588.52	523.63	75	5,357.14
40	358.76	589.04	80	5,714.29
45	230.62	522.44	85	6,071.43
50	145.99	258.39	90	6,428.50
55	96.16	136.08	85	6071.53

Table 7.2 is a systematic representation of the variations of peak wavelengths (WL) and confinement loss (CL) in the healthy and unhealthy refractive indices

with respect to the thickness of gold, as observed in the figure. From the figure, it is interpreted that with the increment of the thickness of the gold layer, the interaction of the incident light with the analyte gets minimized, which results in decrement in the peak loss. Whereas, thin layer of gold disrupts the sensor performance due to high confinement loss. From the table it is clear that out of all the thicknesses, 50nm gold has the maximum change in the wavelength (ΔWL) which delivers maximum sensitivity. With the increase in the t_g, the peak loss value is decreased. Therefore, the optimum thickness for gold will be taken as **50nm,** which shows a moderate loss magnitude for convenient

7.5.1.2. TiO_2 Thickness Optimisation

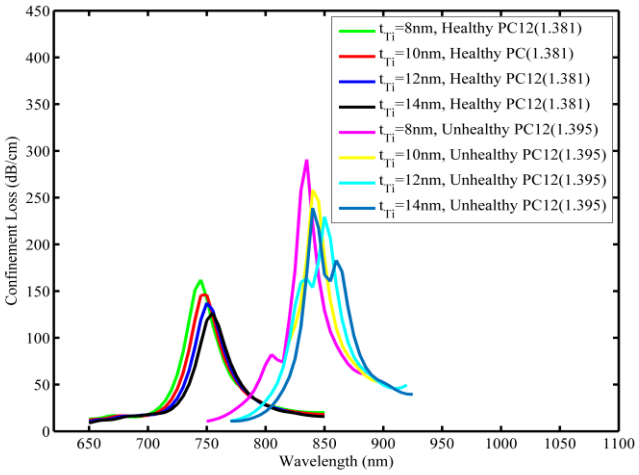

Fig. 7.4 CL Spectra for Various TiO_2 Thicknesses at RI of 1.385 and 1.391

TiO_2 is known as a remarkable plasmonic material that would definitely alter the sensor's performance. The optimal thickness of the TiO_2 (t_{Ti}) is determined by varying it in the range of 8 nm-14 nm at a difference of 2 nm keeping the gold thickness optimal at 50 nm. Figure 4 depict the graph of confinement loss versus the wavelength with the varying thicknesses. Table 7.3 is a systematic representation of the variations of wavelengths and confinement loss (CL) in the healthy and unhealthy refractive indices with respect to the thickness of TiO_2 (t_{Ti}). Since, TiO_2 is applied as sensitivity enhancer and as an adhesive, therefore it has minor influence on the confinement loss. The confinement loss suffers minor decrement with the increase of thickness of TiO_2. In addition, thicker layer tends

to generates some extra loss peaks which should be avoided for appropriate sensing performance. From the table it is clear that, out of all the thicknesses 12 nm has the maximum change in the wavelength (ΔWL). Optimising the thickness of Titanium Dioxide increased the wavelength sensitivity from 6,428.571 nm/RIU to 7142.857 nm/RIU. Therefore, the optimum thickness for further analysis of TiO_2 be 12 nm**.**

Table 7.3
Optimisation of Thickness of TiO_2 Layer

t_{Ti} **(nm)**	**Max. CL (Normal cell) (dB/cm)**	**Max. CL (Infected cell) (dB/cm)**	**ΔWL (nm)**	**Sensitivity (nm/RIU)**
8	162.03	290.82	90	6,428.57
10	145.99	258.39	90	6,428.57
12	137.25	229.42	100	7,142.86
14	126.56	238.82	85	6,071.53

In the proposed biosensor, two types of oblong air holes are present where one is dependent on the other. Optimal width and height of the oblong air hole will be determined in this section, as these air holes are highly responsible for altering the sensitivity. Here the height and width of the air hole will be varied keeping the optimal thickness of gold and TiO_2 as 50nm and 12nm respectively

7.5.1.3. Width (W) Optimization

The optimal width of the oblong air hole is determined by varying it in the range of 1.05 µm -1.15 µm at a difference of 0.05 µm. Figure 7.5 depict the graphical representation of confinement loss versus the wavelength with the varying width.

Table 7.4 displays the systematic representation of the variations of wavelengths and confinement loss (CL) in the healthy and unhealthy refractive indices with respect to the width of oblong air hole (WL).

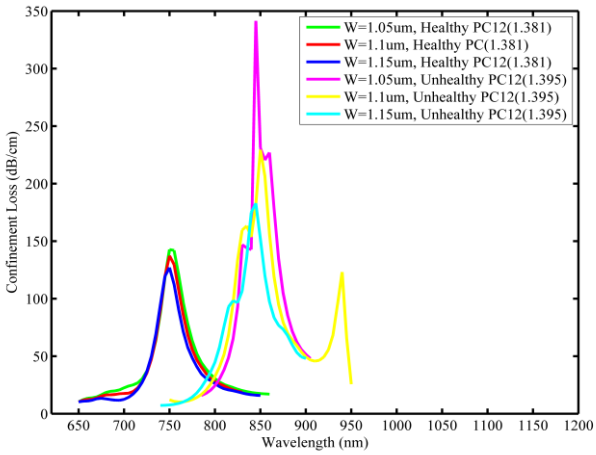

Fig. 7.5 CL spectra for Various Width of the Oblong Air Hole (W) at RI of 1.385 and 1.391

Table 7.4
Optimisation of Width of the Oblong Air Hole (W)

W (µm)	Max. CL (Normal cell) (dB/cm)	Max. CL (Infected cell) (dB/cm)	ΔWL (nm)	Sensitivity (nm/RIU)
1.05	142.66	341.43	90	6,428.57
1.1	137.25	229.43	100	7,142.86
1.15	126.97	182.92	95	6,785.71

As the width increases from 1.05 µm to 1.15 µm the light confinement gets stronger in the core and made it difficult to reach towards the plasmonic material, which eventually reduces the interaction between the core and the plasmon mode, ultimately minimize the confinement loss and affects the sensitivity. From the table it is clear that out of all the width values, 1.1µm has the maximum change in the wavelength (ΔWL). Therefore 1.1 µm width is taken as optimal magnitude for further analysis.

7.5.1.4. Height (H) Optimization

The optimal height of the oblong air hole is determined by varying it in the range of 1.9 µm - 2.1 µm at a difference of 0.05 µm. Figure 7.6 and Table 7.5 provides the systematic representation of the variations of confinement loss with wavelength in the healthy and unhealthy refractive indices with respect to the

height of oblong air hole. From 1.85 µm to 2.05 µm, no major obstruction is faced by core mode to make a proper interaction with the plasmon mode ultimately shows no change in the observed sensitivity with minor decrement in the confinement loss since, increasing height especially upper oblong air holes blocks the core mode to interact with SPP mode. Therefore, to ensure a nominal confinement loss, 2 µm height is taken as optimized value.

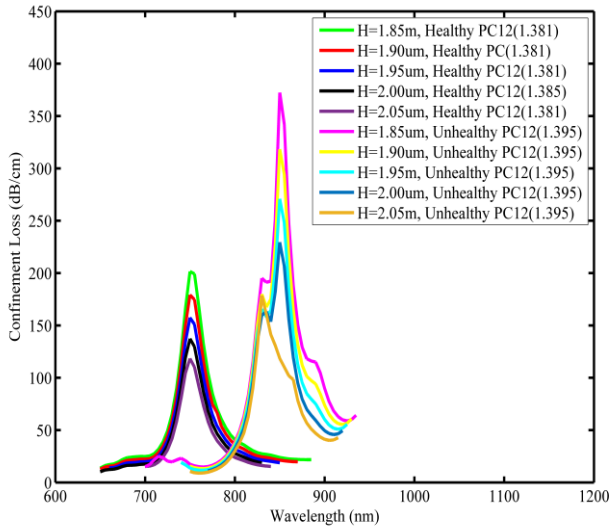

Fig .7.6 CL Spectra for Various Height of the Oblong Air hole H at RI of 1.385 and 1.391

Table 7.5
Optimisation of Height of the Oblong Air Hole (H)

H (µm)	**Max. CL (Normal cell) (dB/cm)**	**Max. CL (Infected cell) (dB/cm)**	**ΔWL (nm)**	**Sensitivity (nm/RIU)**
1.85	201.50	372.33	100	7,142.86
1.90	179.14	318.27	100	7,142.86
1.95	157.42	270.85	100	7,142.86
2.0	137.24	229.42	100	7,142.86
2.05	118.3138	178.46	80	5,714.29

7.5.1.4 Circular Hole Radius (r) Optimization

The optimal radius of the circular air hole is determined by varying it in the range of 0.35 µm – 0.45 µm at a gap of 0.05 µm. Figure 7.7 along with table 6 shows the systematic representation of the variations in the confinement loss in the healthy and unhealthy refractive indices with respect to the width of circular air hole. As it is noticeable from the table that all the radius corresponds to the same change in the peak wavelength with negligible variation in loss, that is because the circular air holes are not playing major role in interaction of the light with the plasmonic materials and also are not connected in any way with the core They are just placed to obstruct the core field from leaking outside core region. Therefore, by maintaining a nominal loss and fabrication possibilities, 0.4 µm is considered as the optimum radius.

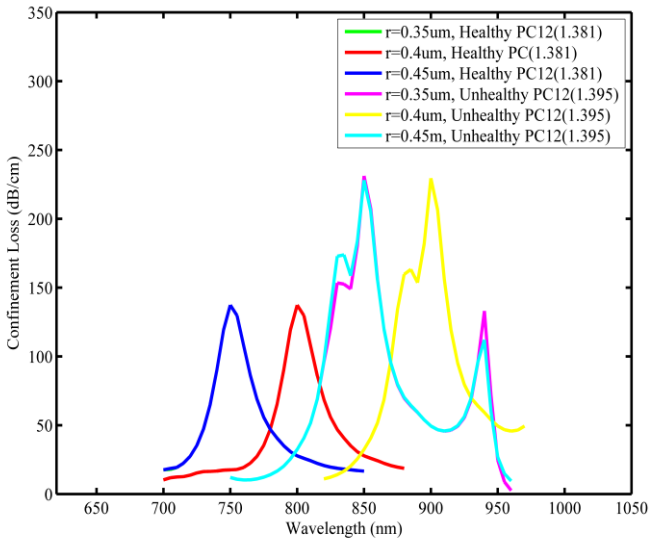

Fig. 7.7 CL Spectra for Various Radius of the Circular Air Hole (r) at RI of 1.385 and 1.391

Table 7.6
Optimisation of Radius of Circular Holes (r)

r (μm)	Max. CL (Normal cell) (dB/cm)	Max. CL (Infected cell) (dB/cm)	ΔWL (nm)	Sensitivity (nm/RIU)
0.35	137.26	231.10	100	7,142.86
0.4	137.24	229.42	100	7,142.86
0.45	137.23	228.01	100	7,142.86

7.5.1.5. Black Phosphorus (BP) optimisation

Black phosphorus are thin layers of 2-D plasmonic material that has a fixed monolayer thickness of 0.53 μm. Here in this section, number of BP layers used will be optimised. As the thickness is very small, the range of the thickness used is 5-9 layers at a difference of 2. Figure 7.8 shows the change in confinement loss versus wavelength with the varying BP layers.

When black phosphorus layers are increased, the sensitivity of the sensor increases rapidly but the FWHM (Full Width Half Maximum) also increases. From table 7.7, it is observed that sensitivity increases in the beginning and then decreases with the increase in the number of layers of BP. Therefore, the optimum number of layers for black phosphorus for the proposed biosensor will be taken as 7 (seven).

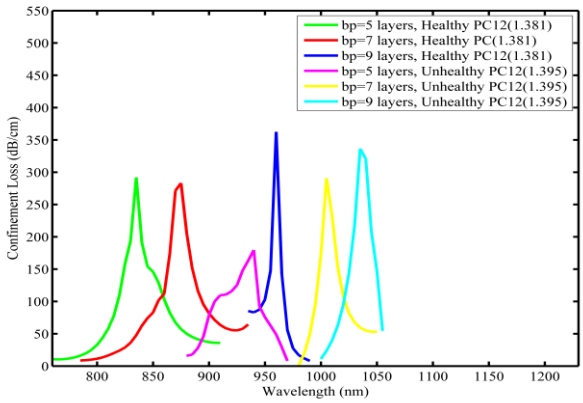

Fig. 7.8. CL Spectra for Various Number of Layers of BP at RI of 1.385 and 1.391

Table 7.7
Optimisation of Number of BP Layers (BP)

No. of BP layers (bp)	Max. CL (Normal cell) (dB/cm)	Max. CL (Infected cell) (dB/cm)	ΔWL (nm)	Sensitivity (nm/RIU)
5	108.37	192.39	100	7,142.86
7	283.12	290.81	130	9,285.71
9	362.55	336.34	75	5,357.14

7.5.2. Sensor Performance

While studying the sensitivity analysis at different cancer cell through the presented PCF SPR sensor, different sets of loss spectrum were found which are listed in the fig 7.9 (a) to (f). In the figure, we have marked the spectra for healthy cells in blue and infected cells in red. It can be seen evidently that all the cells have gone through a wavelength shift, when infected counter parts are associated. The wavelength shift for PC12 is observed as130 nm, for Jurkat (~85 nm), for basal cell (~95 nm), for HeLa (~130nm), for MCF-7, we calculated a shift of 160 nm, and for MDA-MB-231 cell, the respective shift is 150 nm. The former data provides a sensitivity of 9285.71 nm/RIU, 6071.43nm/RIU, 4750nm/RIU, 5416.67nm/RIU, 11,429nm/RIU, 10,714nm/RIU respectively. The BP layers increased the sensitivity by 30%. This shows that the proposed biosensor is suitable for cancer detection.

Table 7.8 represents the comparison of this work with the recently published work to give a clear view on the reliability of the sensor. This proves that the proposed sensor can detect any minute change in the refractive index in the cell of a human body and gives required sign of any cancerous presence.

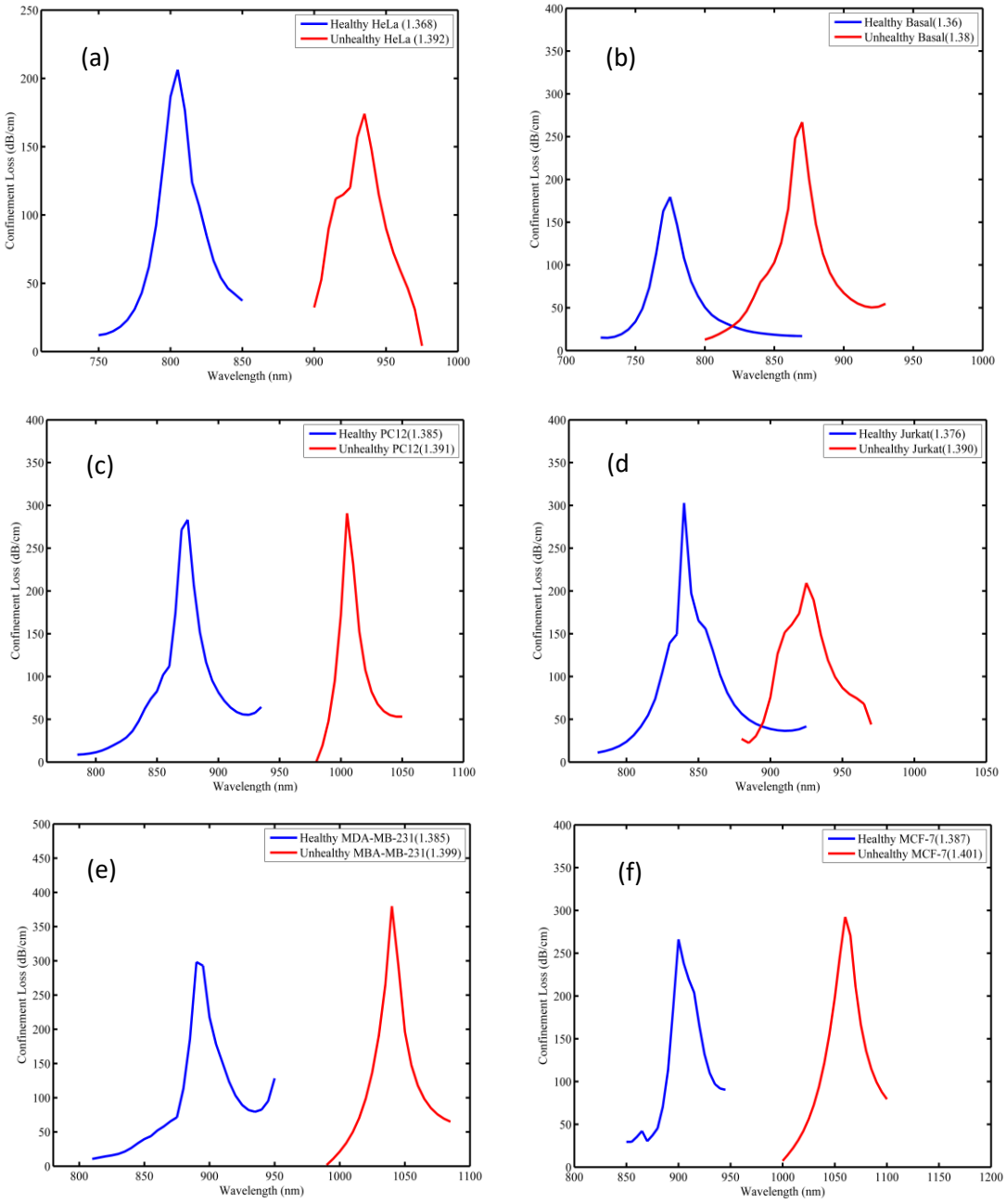

Fig.7.9 Loss Spectra of (a) HeLa (Cervical Cancer); (b) Basal Cell (Skin Cancer); (c) PC12 (Adrenal Gland); (d) Jurkat (Blood Cancer); (e) MDA-MB-231(Breast Cancer Type-1); (f) MCF-7 (Breast Cancer Type-1)

Table 7.8
Comparison of Proposed Work with Past Research Works

Reference	Cancer Type	Wavelength Sensitivity(nm/RIU)
[10]	Skin	3,500
	Cervical	5,000
	Blood	5,714
	Adrenal Gland	6,429
	Breast Type-1	7,143
	Breast Type-2	7,143
[11]	Skin	3,150
	Cervical	4,333.33
	Blood	4,642.86
	Adrenal Gland	5,500
	Breast Type-1	6,428.57
	Breast Type-2	7,142.86
[12]	Skin	3,750
	Cervical	5,417
	Blood	6,071
	Adrenal Gland	7,500
	Breast Type-1	9,643
	Breast Type-2	11,429
[13]	Skin	--
	Cervical	5500
	Blood	6000
	Adrenal Gland	7571.43
	Breast Type-1	9428.57
	Breast Type-2	10714.28
[34]	Skin	3800
	Cervical	5008.33
	Blood	--
	Adrenal Gland	--
	Breast Type-1	6214.28
	Breast Type-2	--
Proposed PCF SPR sensor	**Skin**	**4,750**
	Cervical	**5417**
	Blood	**6071**
	Adrenal Gland	**9286**
	Breast Type-1	**10,714**
	Breast Type-2	**11,429**

7.6. CONCLUSION

The proposed slotted PCF SPR sensor is designed with two types of oblong air holes and circular air holes that shows a high sensitivity towards detection of cancerous cells. In the proposed sensor a 50nm thick layer of Gold and 7 layers of Black Phosphorus with a monolayer thickness of 0.53nm is used as plasmonic materials. Titanium Dioxide (TiO_2) is used as an adhesive between the fiber and gold having thickness (~12 nm), but it also has remarkable plasmonic properties leading to its contribution in the enhancement of sensitivity. COMSOL Multipurpose software is used to determine the sensor's performance using finite element method (FEM). All the different parameters involved in the calculations are optimised to achieve the atmost accuracy. The proposed sensor can detect six kinds of cancer cells (PC12, HeLa, MDA-MB-231, Jurkat, basal, MCF-7). The sensor achieves a very high sensitivity of MCF-7 for the cell 11,429 nm/RIU.

CHAPTER 8

DESIGN AND ANALYSIS OF BLACK PHOSPHORUS LAYERED SPR-PCF BIOSENSOR FOR DETECTION OF CANCER CELLS[2]

8.1. INTRODUCTION

Cancer is one of the most prominent diseases for millions of deaths. It is estimated to have 9.6 million deaths due to cancer [48], [49]. The rapid growth of aberrant cells, which surpasses the normal limit, causes Cancer. When genetic as well as epigenetic alterations occurs in the somatic cells which results in abnormal growth in the cells. Our body is made up of millions of cells, these cells get changed. Our body has a mechanism which requires signals to the brain from each cell. When there is a missing signal the brain starts multiplying cells abruptly, which forms a lump or a tumor. But some cancers do not form a solid lump but they start with the help of bloodstream. This can spread all over the body as these cells penetrate skin tissues and infect nearby organs. Early cancer detection saves a lot of lives, time, and money. On the other hand, traditional detection techniques for cancer are very expensive and, most importantly, less accurate. Therefore, a better counterpart of these sensors should be adopted to make sensing more reliable and economical and so, researchers, scientists, and doctors are trying to find a way out of this painful illness.

The phenomena in which light hits the surface of a metal like Gold, Aluminium, etc., at a certain angle, electrons at the metal surface start to oscillate; these oscillating electrons are known as “Surface Plasmons”. When the oscillating frequency matches the frequency of the incident light, surface plasmon resonance takes place. Photonic Crystal Fiber (PCF) structures have a periodic structure of air

[2] A part of this chapter has been presented in 16th International Conference on Fiber Optics and Photonics (PHOTONICS) 2024, 12-15th December 2024, IIT Kharagpur, West Bengal, INDIA. The full length paper is communicated for the same.

holes within the cladding to confine light better than traditional fibers. This structure helps to create unique properties that are hardly found in traditional fibers such as tailored dispersion characteristics, high birefringence, and enhanced nonlinearity. So, on combining the two aspects, one can get a very efficient fiber sensor that can yield us enhanced results. Generally, these sensors are made up of circular lattice [50]. In this proposed work, we have proposed a D-shaped PCF SPR sensor. The design consists three cubical air holes and spherical air holes with two different diameters. Cubical air holes are currently being worked on in recent literatures and capable of showing amazing results [51]. A Gold layer is used as a plasmonic material which shows a narrow and sharp loss curve, and hence shows clearer and higher wavelength sensitivities. TiO_2 layer is used as an adhesive between the fiber and the gold layer, and due to this, Au is found to be less prone to biomolecule adsorption. 7 layers of Black Phosphorus with monolayer thickness 0.53nm, is also used enhance the sensitivity. BP is a new type of 2-D material which is stacked on the top of the fiber as multiple layers. It increases the sensitivity by attracting larger number of infected cells from the analyte.

8.2. PROPOSED PCF DESIGN

The structure of proposed SPR-PCF sensor is shown in Fig. 1. It consists of three types of air holes are distributed in the cladding, that are cubical air holes with sides l=2 µm and two types of spherical air holes with diameters d1=0.8 µm and d2=0.4 µm. A plasmonic metal layer of Gold and TiO2 is placed above the flat surface of the sensor design. The thickness of gold film used is 30 nm and the thickness of TiO_2 is 10 nm, where it is used as an adhesive between the structure and gold layer. A definite number of Black Phosphorus layers are placed above the gold layer to increase the sensitivity of the sensor to detect cancer cells. The thickness of one layer of BP is taken as 0.53nm, and 7 such layers are used. An analyte layer of thickness a = 1 µm and Perfectly Matched Layer in cylindrical geometry of thickness p = 1.2µm is used. The refractive index of the measured medium, that is analyte is defined as n_a.

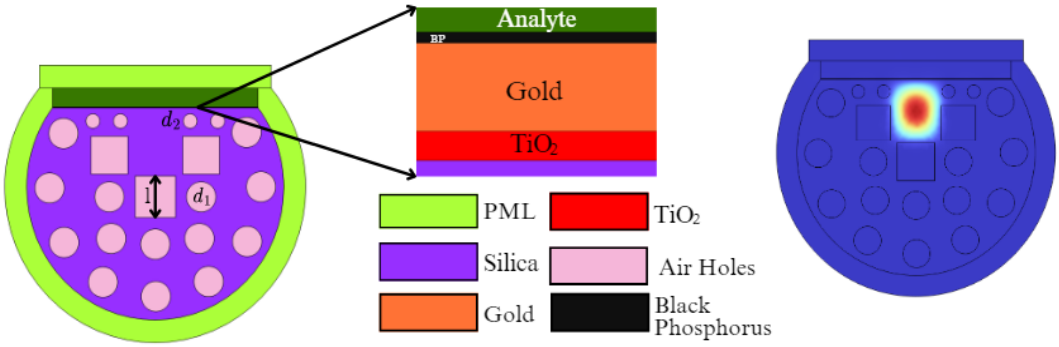

Fig. 8.1 Proposed PCF SPR Sensor (left) Resonant Mode Field at 0.63 μm (right)

The dielectric constant of the Plasmonic material that is gold is calculated using the Drude Lorentz Dispersion Model, which is then used to find refractive index of gold [46, 51],

$$\epsilon_{Au} = \epsilon_{\infty} - \frac{\omega_D^2}{\omega(\omega + j\gamma_D)} - \frac{\Delta\epsilon\,\Omega_L^2}{\omega^2 - \Omega_L^2 + j\Gamma_L\omega} \tag{8.1}$$

Here, ϵ_{∞} is the permittivity at high frequency with magnitude 5.9673. γ_D is the damping factor for free electrons with magnitude ~ $2\pi \times 15.92$ THz, ω_D (~ $2\pi \times 2113.6$ THz) is the frequency by which the free electrons move in a metal when interrupted by light. ω is the frequency of light, or in case if an RI sensor, it is dependent on wavelength of light. Γ_L (~ $2\pi \times 104.86$ THz) is the damping factor for bound electrons, Ω_L (~ $2\pi \times 650.07$ THz) is the frequency of bound electrons which are vibrating when light disturbs them, and $\Delta\epsilon$ is the change in permittivity due to vibration of bound electrons.

Fused Silica is used as a base material of sensor and PML, whose RI can be determined by the Sellmeier equation, because Fused Silica's refractive index is wavelength dependent.

$$n^2(\lambda) = 1 + \frac{B_1\lambda^2}{\lambda^2 - C_1} + \frac{B_2\lambda^2}{\lambda^2 - C_2} + \frac{B_3\lambda^2}{\lambda^2 - C_3} \tag{8.2}$$

where λ is the wavelength of light and B_1=0.696163, B_2=0.4079426, B_3 =0.8974794, C_1=0.0684043, C_2=0.1162414, C_3=9.896161 are constants.

A thin layer of TiO_2 acts as an adhesive between PCF structure and plasmonic material that is gold here. The RI of TiO_2 is calculated using the following formula, where λ is in the Å units:

$$n^2 = 5.913 + \frac{0.2441}{\lambda^2 - 0.0803} \tag{8.3}$$

The RI of Black Phosphorus is calculated using the Cauchy absorbent formula in which λ is taken in nm units. The following equation gives the real and imaginary parts of R.I of BP [38],

$$\mathrm{n}(\lambda) = \mathrm{A} + \mathrm{B}\frac{10^4}{\lambda^2} + \mathrm{C}\frac{10^9}{\lambda^4} \tag{8.4}$$

$$\mathrm{k}(\lambda) = \mathrm{D} \times 10^{-5} + \mathrm{E}\frac{10^4}{\lambda^2} + \mathrm{F}\frac{10^9}{\lambda^4} \tag{8.5}$$

Here, n(λ), and k(λ) are the real and imaginary part of the refractive index respectively, and A=3.57, B=6.79, C=39.99, D=3206, E=-0.521, and F=10.26 are constants.

The confinement loss which tells about the amount light leaked from the PCF core can be calculated using the previously explained equation 6.2.

The performance of the sensor is calculated with the help of wavelength sensitivity, using the following equation,

$$\mathrm{S_w(nm/RIU)} = \frac{\Delta\lambda_{\mathrm{peak}}}{\Delta \mathrm{n_a}} \tag{8.6}$$

where, $\Delta\lambda_{\mathrm{peak}}$ is the change in peak wavelength when effective RI is changed around the PCF and $\Delta \mathrm{n_a}$ is the change in refractive index of analyte.

8.3. RESULTS AND DISCUSIONS

We have examined the three cancer cells, which consists of blood, skin and cervical cancerous components named Jurkat, Basal, HeLa cell respectively. The respective loss profiles are displayed in fig. 2. The enhanced sensitivity is observed for both the scenarios. The blood cancer cell is detectable with sensitivity of 7142.86 nm/RIU, skin cancer cell can be sensed at wavelength sensitivity of 5000 nm/RIU and similarly, cervical cancer can be detected with 8333.33 nm/RIU of wavelength sensitivity.

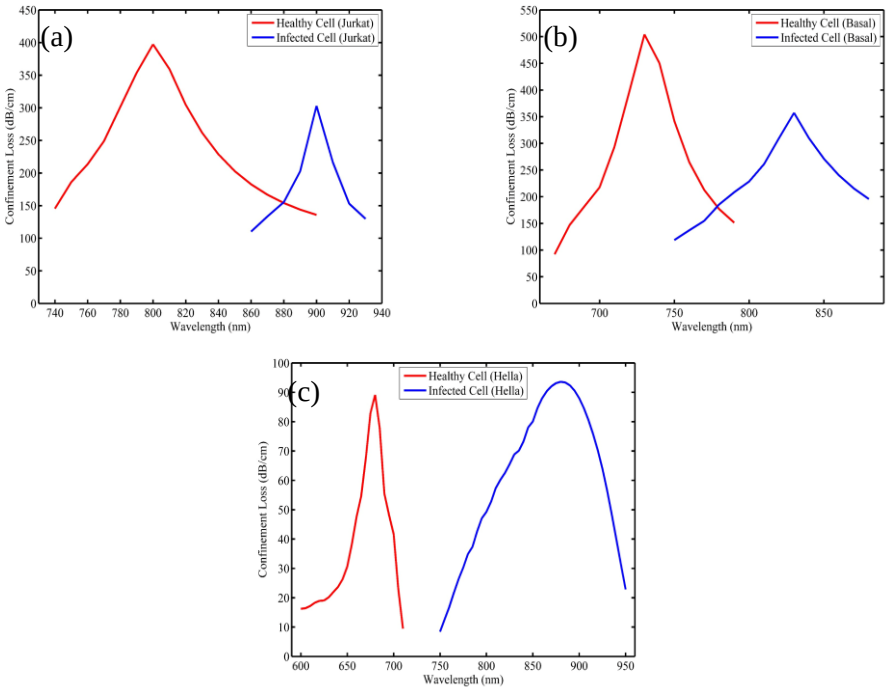

Fig. 8.2 Loss Profile of Healthy and Infected Cell of (a) Jurkat (b) Basal (c) HeLa

Table 1 shows the comparison of proposed sensor with some previous works published in past years. The table also contains the refractive indices of healthy and infected cells of respective cancer cells which are required to do the simulations on the SPR-PCF sensor.

Table 8.2
Performance of Proposed Cancer Cell SPR based PCF Sensor.

PCF Design	Cell Name	RI of Cells		Sensitivity (nm/RIU)
		Healthy Cell	Infected cell	
Dual Core Double Polished PCF-SPR [52]	Jurkat	1.376	1.390	5714
	Basal	1.36	1.38	3500
	HeLa	1.368	1.392	5000
Dual Core PCF Biosensor [53]	Jurkat	1.376	1.390	6071
	Basal	1.36	1.38	3750
	HeLa	1.368	1.392	5417
Proposed Sensor	Jurkat	1.376	1.390	7142.86
	Basal	1.36	1.38	5000
	HeLa	1.368	1.392	8333.33

8.4. Conclusions

A D-shaped SPR based PCF biosensor is designed with cubical and spherical air holes to detect blood (Jurkat), skin (Basal) and cervical (HeLa) cancer. Au film as a plasmonic material and TiO2 as an adhesive and 7 layers of BP have been used to enhance the sensing power of the biosensor. The sensor is able to achieve sensitivity of 7142.86 nm/RIU, 5000 nm/RIU and 8333.33 nm/RIU for Jurkat, Basal and Hella cells. respectively. So, it can be used as better counterpart in cancer sensing.

CHAPTER 9

CONCLUSION AND SCOPE FOR FUTURE WORK

➢ CONCLUSION

In this work, we have studied and designed Surface Plasmon Resonance based Photonic Crystal Fiber to detect cancer with biosensing approach. The proposed sensors are refractive index sensor, which when subjected to change in refractive index of an analyte can show high sensitivity. Different types of airholes are used to explore their impact on the sensors performance. Oblong air holes and rectangular air holes are used in different configurations and a special 2D plasmonic material called black phosphorous is used along with gold and TiO_2 to detect different cancer cells including blood cancer, cervical cancer, adrenal gland cancer, breast cancer type I and type II. They are then simulated and numerically analysed in COMSOL Multiphysics software to analyse all the required optical properties of both the proposed designs.

➢ SCOPE FOR FUTURE WORK

In the research work further, I shall work on the following topics:

1. Using the COMSOL Multiphysics software, my sole aim is to focus on designing of PCF Sensors based on SPR for the detection of cancer cell.

2. Second priority is set to obtain maximum sensitivity.

3. In the future, I am intending to work on different other emerging plasmonic material such as Germanene, Graphene, MoS_2, MXenes, etc., over a vast number of biological applications. To understand the further improvement of medical analysis og such diseases in all aspects possible.

REFERENCES

[1] Krauss, Thomas F., et al. "Photonic crystals in the optical regime—past, present and future." *Progress in Quantum electronics* 23(2) (1999): 51-96.

[2] Xia, Changming, et al. "Fabrication and laser performance of Yb3+/Al3+ co-doped photonic crystal fiber synthesized by plasma nonchemical vapor deposition method." *Optical fiber technology* 25 (2015): 20-24.

[3] Rifat, Ahmmed A., et al. "Development of photonic crystal fiber-based gas/chemical sensors." *Computational photonic sensors* (2019): 287-317.

[4] Chemnitz, Mario et al. "Liquid-Core Optical Fibers—A Dynamic Platform for Nonlinear Photonics." *Laser & Photonics Reviews* 17(9) (2023): 2300126.

[5] Chow, Desmond M., et al. "Fabrication of photonic crystal fibers." *2012 Ieee 3rd international conference on photonics*. IEEE, (2012).

[6] Kaur, Baljinder, et al. "Recent advancements in optical biosensors for cancer detection." *Biosensors and Bioelectronics* 197 (2022): 113805.

[7] Khamaru, Akash, et al. "As38 Se62 based segmented clad-graded index photonic crystal fiber for supercontinuum generation covering 3–9.5 μm with moderate peak power." *Optical and Quantum Electronics* 56(7) (2024): 1246.

[8] Gangwar, Rahul Kumar, et al. "High performance titanium oxide coated D-shaped optical fiber plasmonic sensor." *IEEE sensors journal* 19(20) (2019): 9244-9248.

[9]May-Arrioja, Daniel A., et al. "Photonic Crystal Fibers for Sensing Applications." *Photonic Crystal and Its Applications for Next Generation Systems*. Singapore: Springer Nature Singapore, 2023. 155-170.

[10] Arya, Neel Kumar, et al. "Design and analysis of low loss porous-core photonic crystal fiber for terahertz wave transmission." *Materials Today: Proceedings* 80 (2023): 1797-1800.

[11] Bise, Ryan T., et al. "Sol-gel derived microstructured fiber: fabrication and characterization." *Optical fiber communication conference* 3 (2005).

[12] Ghazanfari, Amir, et al. "A novel freeform extrusion fabrication process for producing solid ceramic components with uniform layered radiation drying." *Additive Manufacturing* 15 (2017): 102-112.

[13] Bao, Hualong, et al. "Fabrication and characterization of porous-core honeycomb bandgap THz fibers." *Optics express* 20(28) (2012): 29507-29517.

[14] Ebendorff-Heidepriem, Heike, et al. "3D-printed extrusion dies: a versatile approach to optical material processing." *Optical Materials Express* 4(8) (2014): 1494-1504.

[15] Rahman, KM Mustafizur, M. Shah Alam, and M. Asiful Islam. "Highly sensitive gold-coated surface plasmon resonance photonic crystal fiber sensor in near-infrared region." *Results in Optics* 7 (2022): 100223.

[16] Aftab, Muhammad, et al. "Surface plasmon excitation: theory, configurations, and applications." *Plasmonics* 19(4) (2024): 1701-1719.

[17] Liang, Han, et al. "High-performance PCF-SPR sensor coated with Ag and graphene for humidity sensing." *Plasmonics* 17(4) (2022): 1765-1773.

[18] Tong, Kai, et al. "Study on increasing measurement range and enhancing sensitivity of PCF surface-plasmon-resonance biosensor using black phosphorus." *Journal of Russian Laser Research* 42 (2021): 283-291.

[19] Zhang, Guowei, et al. "Layer-Dependent Electronic and Optical Properties of 2D Black Phosphorus: Fundamentals and Engineering." *Laser & Photonics Reviews* 15(6) (2021): 2000399.

[20] Castellanos-Gomez, Andres, et al. "Isolation and characterization of few-layer black phosphorus." *2D Materials* 1(2) (2014): 025001.

[21] Kaushansky, Kenneth, et al. McGraw-Hill Education, 2016.Das, Sreyashi, et al. "Surface plasmon resonance (SPR) sensor for cancer biomarker detection." *Biosensors* 13(3) (2023): 396.

[22] Karki, Bhishma, et al. "Advances in Surface Plasmon Resonance-Based Biosensor Technologies for Cancer Cell Detection." *International Journal of Optics* 2022(1) (2022): 1476254.

[23] Ayyanar, N., et al. "Photonic crystal fiber-based refractive index sensor for early detection of cancer." *IEEE sensors journal* 18(17) (2018): 7093-7099.

[24] Jabin, Md Asaduzzaman, et al. "Surface plasmon resonance based titanium coated biosensor for cancer cell detection." *IEEE Photonics Journal* 11(4) (2019): 1-10.

[25] Panda, Abinash, et al. "Design and analysis of porous core photonic crystal fiber based ethylene glycol sensor operated at infrared wavelengths." *Journal of computational electronics* 20 (2021): 943-957.

[26] Arif, Md Faizul Huq, et al. "Design and optimization of photonic crystal fiber for liquid sensing applications." *Photonic Sensors* 6 (2016): 279-288.

[27] Xu, Huizhen, et al. "High numerical aperture photonic crystal fiber with silicon nanocrystals core for optical coherence tomography." *Optik* 219 (2020): 165000.

[28] Sen, Shuvo, et al. "Zeonex based decagonal photonic crystal fiber (D-PCF) in the terahertz (THz) band for chemical sensing applications." *Sensing and Bio-Sensing Research* 31 (2021): 100393.

[29] Labi, V., et al. "How cell death shapes cancer." *Cell death & disease* 6(3) (2015): e1675-e1675.

[30] Saini, Anupam, et al. "Cancer causes and treatments." *Int J Pharm Sci Res* 11(7) (2020): 3121-3134.

[31] Mittal, Sunil, et al. "Biosensors for breast cancer diagnosis: A review of bioreceptors, biotransducers and signal amplification strategies." *Biosensors and Bioelectronics* 88 (2017): 217-231.

[32] Venkatram, Prabhakar. "Other Diagnostic modalities, advantages and disadvantages in different pathologic conditions." *Heart Diseases and Echocardiogram: Principles in Practice*. Cham: Springer Nature Switzerland, 2024. 783-787.

[33] Rankin, Sheila C. "CT and MRI." *Surgery (Oxford)* 23(5) (2005): 162-165.

[34] Zuhayer, Asif, et al. "A gold-plated twin core d-formed photonic crystal fiber (PCF) for ultrahigh sensitive applications based on surface plasmon resonance (SPR) approach." *Plasmonics* 17(5) (2022): 2089-2101.

[35] Islam, Nazrul, et al. "Highly sensitive open channel based PCF-SPR sensor for analyte refractive index sensing." *Results in physics* 46 (2023): 106266.

[36] Opoku, Gideon, et al. "Design and numerical analysis of a circular SPR based PCF biosensor for aqueous environments." *Available at SSRN 4355473* (2023).

[37] Lee, Seong-Yeon, et al. "Black phosphorus phase retarder based on anisotropic refractive index dispersion." *2D Materials* 9(1) (2021): 015020.

[38] Pysz, D., et al. "Stack and draw fabrication of soft glass microstructured fiber optics." *Bulletin of the Polish Academy of Sciences. Technical Sciences* 62(4) (2014): 667-682.

[39] Atakaramians, Shaghik. *Terahertz waveguides: a study of microwires and porous fibres*, 2011.

[40] Rifat, Ahmmed A., et al. "Photonic crystal fiber based plasmonic sensors." *Sensors and Actuators B: Chemical* 243 (2017): 311-325.

[41] Boehm, Jonathan, et al. "Chemical deposition of silver for the fabrication of surface plasmon microstructured optical fibre sensors." *Plasmonics* 6 (2011): 133-136.

[42] Boehm, Jonathan, et al. "Chemical deposition of silver for the fabrication of surface plasmon microstructured optical fibre sensors." *Plasmonics* 6 (2011): 133-136.

[43] Nielsen, Kristian, et al. "Selective filling of photonic crystal fibres." *Journal of Optics A: Pure and Applied Optics* 7(8) (2005): L13.

[44] Majeed, Mohammed F., et al. "Design and analysis of a high sensitivity open microchannel PCF-based surface plasmon resonance refractometric sensor." *Optical Materials* 147 (2024): 114617.

[45] Ibrahimi, Khalid Mohd, et al. "Enhance the design and performance analysis of a highly sensitive twin-core PCF SPR biosensor with gold plating for the early detection of cancer cells." *Plasmonics* 18(3) (2023): 995-1006.

[46] Abdelghaffar, M., et al. "Highly sensitive V-shaped SPR PCF biosensor for cancer detection." *Optical and Quantum Electronics* 55(5) (2023): 472.

[47] Ferlay, Jacques, et al. "Cancer incidence and mortality worldwide: sources, methods and major patterns in GLOBOCAN 2012." *International journal of cancer* 136(5) (2015): E359-E386.

[48] Bray, Freddie, et al. "Global cancer statistics 2018: GLOBOCAN estimates of incidence and mortality worldwide for 36 cancers in 185 countries." *CA: a cancer journal for clinicians* 68(6) (2018): 394-424.

[49] Chaudhary, Vijay Shanker, et al. "Au-TiO 2 coated photonic crystal fiber based SPR refractometric sensor for detection of cancerous cells." *IEEE transactions on nanobioscience* 22(3) (2022): 562-569.

[50] Upadhyay, Anurag, et al. "Analysis of proposed PCF with square air hole for revolutionary high birefringence and nonlinearity." *Photonics and Nanostructures-Fundamentals and Applications* 43 (2021): 100896.

[51] Sardar, Md Ranju, et al. "Dual-core dual-polished PCF-SPR sensor for cancer cell detection." *IEEE Sensors Journal* 24(7) (2024): 9843-9854.

[52] Majeed, Mohammed F., et al. "Design and analysis of a dual-core PCF biosensor based on SPR for cancerous cells detection." *Optical and Quantum Electronics* 56(6) (2024): 1030.

APPENDIX 1: PLAGIARISM REPORT

ARHEE BHUYAN

Project Report.docx

Delhi Technological University

Document Details

Submission ID
trn:oid:::27535:99522206

Submission Date
Jun 5, 2025, 9:17 PM GMT+5:30

Download Date
Jun 5, 2025, 9:20 PM GMT+5:30

File Name
Project Report.docx

File Size
25.1 MB

70 Pages

13,217 Words

73,950 Characters

turnitin Page 1 of 75 - Cover Page Submission ID trn:oid:::27535:99522206

APPENDIX 1: PLAGIARISM REPORT

9% Overall Similarity

The combined total of all matches, including overlapping sources, for each database.

Filtered from the Report

- Bibliography
- Quoted Text
- Cited Text
- Small Matches (less than 12 words)

Exclusions

- 1 Excluded Source

Match Groups

60 Not Cited or Quoted 9%
Matches with neither in-text citation nor quotation marks

0 Missing Quotations 0%
Matches that are still very similar to source material

0 Missing Citation 0%
Matches that have quotation marks, but no in-text citation

0 Cited and Quoted 0%
Matches with in-text citation present, but no quotation marks

Top Sources

5% Internet sources
6% Publications
5% Submitted works (Student Papers)

Integrity Flags

2 Integrity Flags for Review

Replaced Characters
6 suspect characters on 4 pages
Letters are swapped with similar characters from another alphabet.

Hidden Text
1 suspect characters on 1 page
Text is altered to blend into the white background of the document.

Our system's algorithms look deeply at a document for any inconsistencies that would set it apart from a normal submission. If we notice something strange, we flag it for you to review.

A Flag is not necessarily an indicator of a problem. However, we'd recommend you focus your attention there for further review.

turnitin Page 2 of 75 - Integrity Overview Submission ID trn:oid:::27535:99522206

APPENDIX 2: RESEARCH PUBLICATION

Plasmonics
https://doi.org/10.1007/s11468-024-02715-5

RESEARCH

Black Phosphorus-Based Slotted D-Shaped PCF SPR Sensor for Cancer Detection

Arhee Bhuyan[1] · Akash Khamaru[1] · Ajeet Kumar[1]

Received: 19 November 2024 / Accepted: 13 December 2024

Abstract
This work proposes a slotted D-shaped photonic crystal fiber (PCF) surface plasmon resonance (SPR) sensor for the detection of cancerous cells. Cancerous analytes are used in different concentrations having different refractive indices (RI) in the sensing medium. To confine the light in PCF, two types of air holes are incorporated, i.e., circular and oblong-shaped air holes. The designed PCF is coated with a gold layer (50 nm) along with TiO_2 (12 nm) that works as a plasmonic enhancer as well as an adhesive to stick the PCF with gold. Apart from gold + TiO_2, an additional seven layers of emerging plasmonic material—black phosphorus are coated on the frame to enhance the sensitivity having a monolayer thickness (0.53 nm). Since healthy and infected cells have different RI, therefore the coupling conditions also differ, which is reflected in peak confinement loss wavelength shift. With the help of the spectral shift, respective wavelength sensitivity (WS) is determined. The WS obtained for cervical, blood, skin, adrenal gland, and breast (types 1 and 2) cancerous cells are 5417 nm/RIU, 6071 nm/RIU, 4750 nm/RIU, 9286 nm/RIU, 11,429 nm/RIU, and 10,714.29 nm/RIU, respectively. The recorded results show that our proposed sensor is a better counterpart among previously proposed sensors and suitable for cancer cell detection.

Keywords Slotted PCF · Black phosphorus · Oblong air holes · Surface plasmon resonance

Introduction

The body is made up of millions of microscopic cells, each of which functions as a completely different living organism. Every single cell in our body works collectively with every other cell to form our tissues and organs. An illustration of this cooperation can be seen in the process by which cell division takes place. They begin to regenerate when it becomes necessary to fix damaged or dead cells. When the process of cellular replication becomes unregulated, cancer develops [1]. Each cell has a nucleus that contains a huge bunch of chromosomes, and these chromosomes are made of genes in the form of DNA strands containing coded messages that guide the cell about the work they will perform. This is how the information about the presence of dead cells reaches the brain, and the cells undergo the process of cell division. During cell division, a mutation occurs which may be the outcome of smoking or any other external harmful factor. The discussed process of cell division gets misled, and without any instructions, cells start to grow abruptly, resulting in the formation of a lump known as cancer [2]. As soon as it is discovered, it is already in a stage where no treatment can help with the recovery. Cancer is actually the growth of cells in an abnormal way which changes the usual gene replication and eventually, it becomes a multiple-cell system that disbalances the cell replication in the body [3]. It ultimately transforms into a huge cell group that can invade any tissues in any part of the body. Through invading tissues, they infect the entire organ system, causing a painful death of the host.

Therefore, early detection of cancerous cells is one of the most talked topic. Generally, people avail detection techniques like MRI (magnetic resonance imaging), PET-CT (positron emission tomography-computed tomography), biopsy, X-ray, and CT scans to monitor cancerous presence

✉ Ajeet Kumar
ajeetdph@dtu.ac.in

Arhee Bhuyan
arheebhuyan_23mscphy72@dtu.ac.in

Akash Khamaru
akashkhamaru_23phdap02@dtu.ac.in

[1] Advanced Photonics Simulation Research Laboratory, Department of Applied Physics, Delhi Technological University, Shahbad Daulatpur, Bawana Road, Delhi 110042, India

Published online: 19 December 2024

APPENDIX 3: CONFERENCE CERTIFICATE

APPENDIX 4: PROOF OF SCIE INDEXING